FOSSIL

DOE/MC/24261-2672
(DE89000926)

Development of Ternary Alloy Cathode Catalysts for Phosphoric Acid Fuel Cells

Final Report

November 1988

Work Performed Under Contract No.: DE-AC21-82MC24261

For
U.S. Department of Energy
Office of Fossil Energy
Morgantown Energy Technology Center
Morgantown, West Virginia

By
Giner, Inc.
Waltham, Massachusetts

DISCLAIMER

DISCLAIMER

Price: Printed Copy A05
Microfiche A01

Printed in the United States of America, Office of Scientific and Technical Information, Oak Ridge , Tennessee

DOE/MC/24261--2672

DE89 000926

Development of Ternary Alloy Cathode Catalysts for Phosphoric Acid Fuel Cells

Final Report

Work Performed Under Contract No.: DE-AC21-82MC24261

For
U.S. Department of Energy
Office of Fossil Energy
Morgantown Energy Technology Center
P.O. Box 880
Morgantown, West Virginia 26507-0880

By
Giner, Inc.
14 Spring Street
Waltham, Massachusetts 02254-9147

November 1988

ABSTRACT

This report presents the results of a five-year program "*Development of Ternary Alloy Cathode Catalysts for Phosphoric Acid Fuel Cells*," performed by Giner, Inc. under Contract DE-AC21-82MC24261, from the Morgantown Energy Technology Center of the U.S. Department of Energy.

The overall objective of the program was the identification, development and incorporation of high activity platinum ternary alloys on corrosion resistant supports, for use in advanced phosphoric acid fuel cells. Two high activity ternary alloys, Pt-Cr-Ce and Pt-Ni-Co, both supported on Vulcan XC-72, were identified during the course of the program. The Pt-Ni-Co system was selected for optimization, including preparation and evaluation on corrosion resistant supports such as 2700°C heat-treated Vulcan XC-72 and 2700°C heat-treated Black Pearls 2000.

A series of tests identified optimum metal ratios, heat-treatment temperatures and heat-treatment atmospheres for the Pt-Ni-Co system. During characterization testing, it was discovered that approximately 50% of the nickel and cobalt present in the starting material could be removed, subsequent to alloy formation, without degrading performance. Extremely stable full cell performance was observed for the Pt-Ni-Co system during a 10,000 hour atmospheric pressure life test.

Several theories are proposed to explain the enhancement in activity due to alloy formation. Recommendations are made for future research in this area.

ACKNOWLEDGMENTS

This work was supported by the Morgantown Energy Technology Center of the U.S. Department of Energy under Contract DE-AC21-82MC24261.

Giner Inc. would like to thank Mr. Robert King of the NASA Lewis Research Center for providing general technical guidance and offering many helpful suggestions which contributed greatly to the success of the program. The suggestions of Mr. Albert Antoine, NASA Lewis, are also appreciated.

The following individuals contributed to this program: V. Jalan, Ph.D., J. Kosek, Ph.D., J. Giner, Ph.D., E.J. Taylor, Ph.D., E. Anderson, V. Bianchi, C. Brooks, K. Cahill, C. Cropley, M. Desai, D. Frost, B. Morriseau, B. Paul, J. Poirier, M. Rousseau, L. Swette, and R. Waterhouse.

TABLE OF CONTENTS

TABLE OF CONTENTS (Continued)

LIST OF TABLES

LIST OF TABLES (Continued)

LIST OF FIGURES

LIST OF FIGURES (Continued)

1.0 INTRODUCTION

The phosphoric acid fuel cell (PAFC) is rapidly approaching commercialization for both dispersed power plant applications and on-site cogeneration applications. In an effort to improve the performance and stability of the PAFC, Giner, Inc., through funding from the U.S. Department of Energy via the NASA Lewis Research Center, undertook a program to develop improved cathode electrocatalysts for use in PAFC's. This program (from July 1982 to March 1988) was based on the development of high activity platinum ternary alloys deposited on carbon supports. During the course of the program we identified and patented a Pt-Ni-Co/carbon platinum ternary alloy which provided improved performance when compared to either platinum or heat-treated platinum cathode electrocatalysts. This electrocatalyst was evaluated under both pressurized (1,000 hours) and atmospheric (10,000 hours) fuel cell conditions (190°C, 100% H_3PO_4, ≥200 mA/cm^2) and was shown to have stable performance.

A large number of binary, ternary and quartenary platinum alloys were prepared and evaluated during the performance of this program; alloying components included both metal and non-metal components. These alloys were characterized with respect to their physical/chemical/electrochemical properties.

Figure 1-1 is an outline of the catalyst development program. An experimental approach was adopted which also involved obtaining an understanding of catalyst operation through careful characterizations. After an initial screening of various catalysts, the most promising were chosen for optimization in terms of performance and stability. In addition to optimizing the catalyst, factors which affect the overall gas diffusion electrode were investigated.

Figure 1-2 is a flow diagram of the experimental portion of the program, showing the steps from the carbon starting material to full cell life testing under both atmospheric and pressurized conditions. As can be seen, catalyst characterization was an important part of the program.

During the course of this program we also developed an empirical relationship which allowed us to predict the composition of additional high activity platinum alloy electrocatalysts; this relationship was used to identify the Pt-Ni-Co system as a potential catalyst.

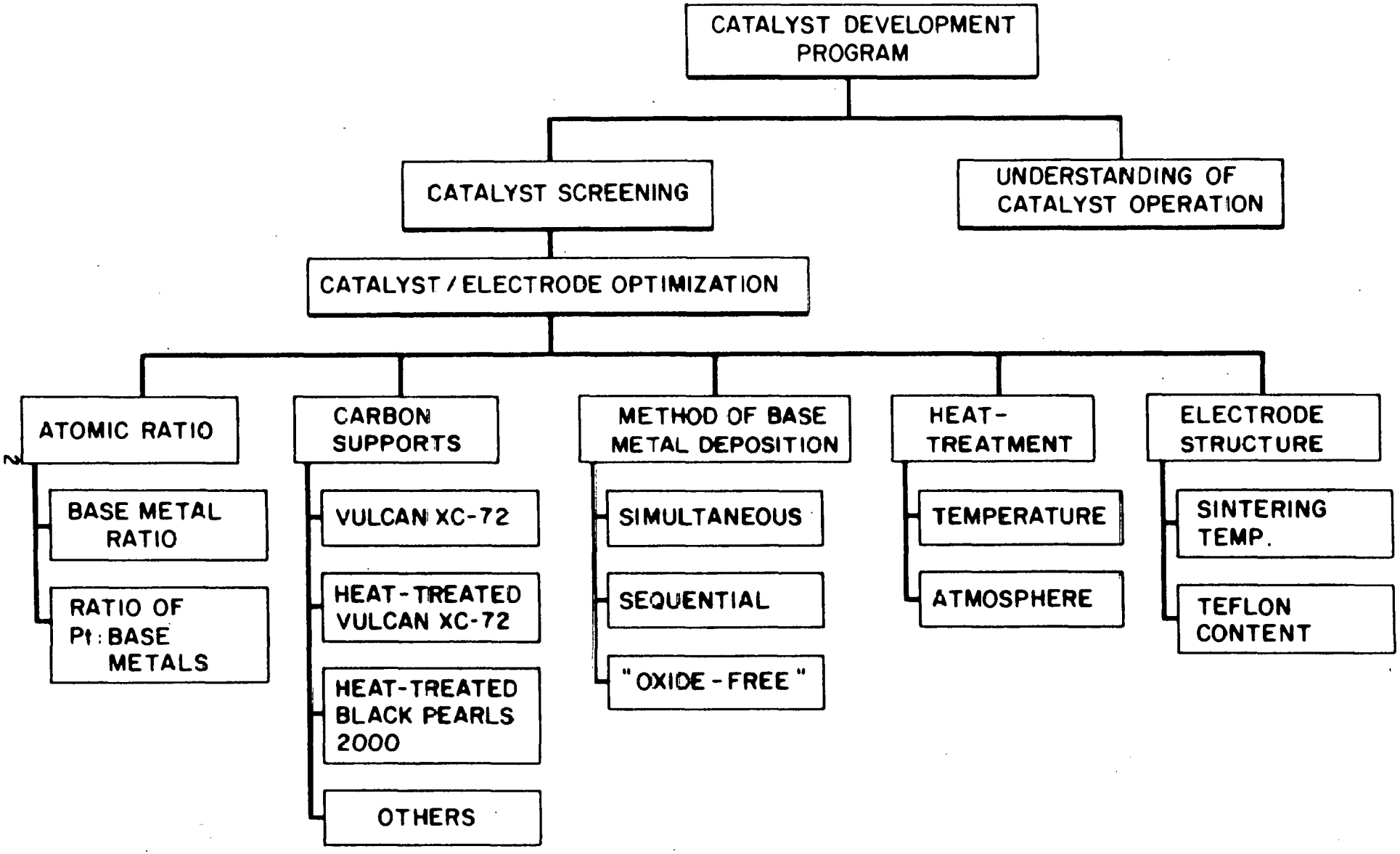

Figure 1-1. Catalyst Development Program Outline

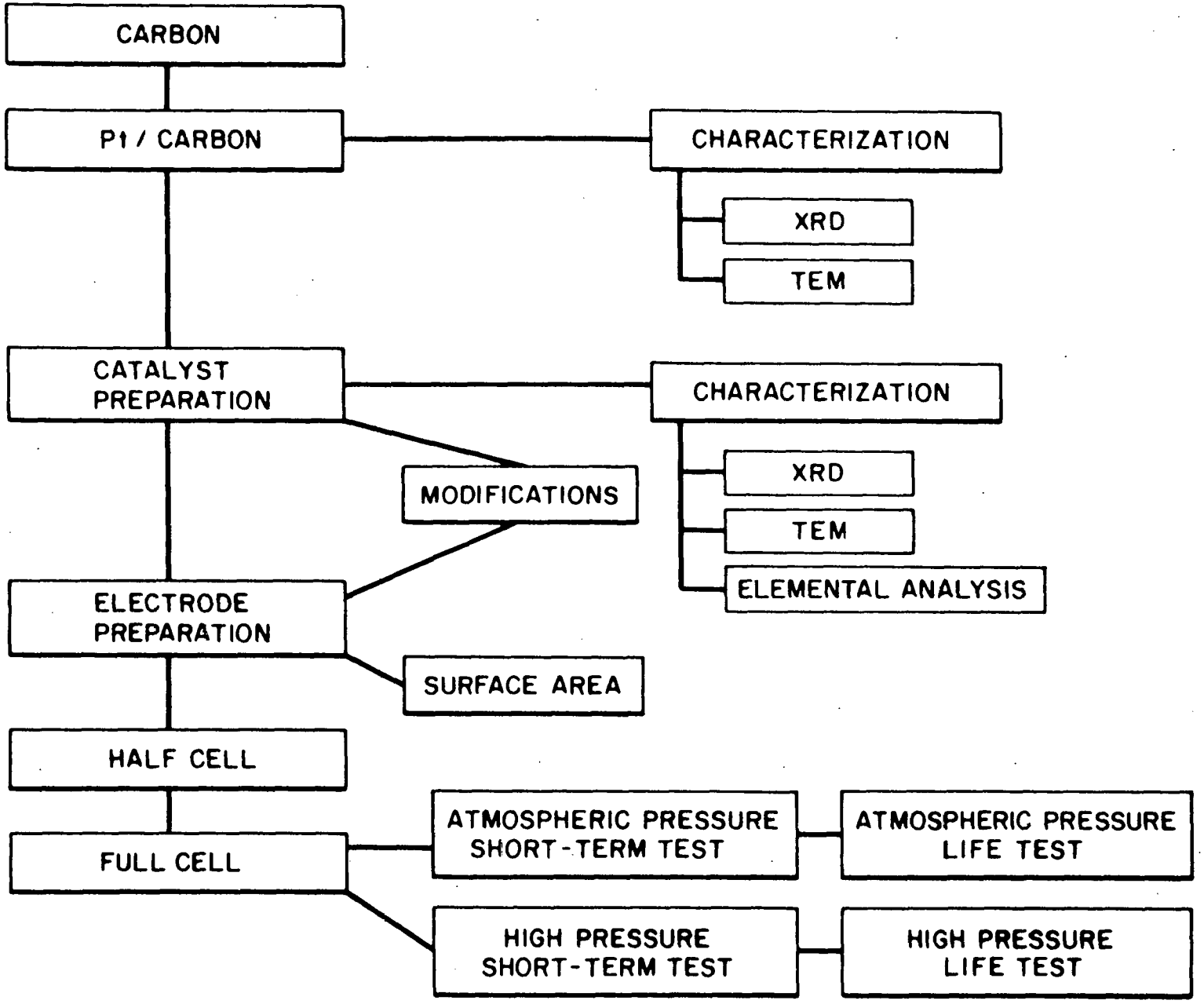

Figure 1-2. Experimental Approach

Due to the harsh conditions the cathode electrocatalyst is subjected to, especially during pressurized fuel cell operation, the identification, preparation and characterization of advanced corrosion-resistant electrocatalyst supports were also undertaken.

Recommendations are made for future research in this area.

2.0 MATERIALS SELECTION

2.1 METALLIC ADDITIVES

The objective of the program was to develop a more efficient fuel cell which can be used without major hardware modification in the phosphoric acid fuel cell power plants already under development. In order to achieve maximum payoff, the program was started by carrying out an advanced study of some already conceived, specific concepts in the area of platinum-containing alloys and platinum compounds to obtain high activity, cost effective catalysts with long life time.

Basically, three approaches could be followed to study and select electrocatalysts: At one extreme, electrocatalytic activity could be selected by relating the activity to physical properties of the catalyst on purely theoretical grounds; at the other extreme, a pragmatic empirical approach could be followed, and materials would be selected by analogies and by extrapolation from other examples of catalysis or electrocatalysis, or in the most empirical approach, by testing any conductive material which was stable under pertinent conditions. We adopted a somewhat intermediate approach in which electrocatalysts were tested for activity and the measured activity correlated to physical parameters of the catalyst. Presumably, once such a correlation had been found, catalysts could be selected by looking at the pertinent physical characteristics.

Based on our prior experience, we initially emphasized the preparation and testing of compounds containing platinum and other elements which had shown some activity for O_2 electro-reduction in acid or, based on some related measurements, were suspected to have some activity. In such compounds, the other elements or groups can play a role in enhancing the catalytic activity and stability of platinum.

Alloying has long been known to alter physiochemical properties such as catalytic activity and selectivity of the constituent components. In fuel cell catalysis, it recently has been shown that many forms of alloying with platinum reduce electrochemical sintering of catalyst crystallites and increase catalytic activity.

Most early work carried out towards the study of alloys for electrocatalysts used smooth or relatively low surface area materials. From the recent research work in hydrocarbon processing, it was evident that small particles of bimetallic materials behaved quite differently from the low surface area materials with the same

constituents. For example, Sinfelt (1) and coworkers have demonstrated unusual changes in activity and selectivity of supported, high surface area, bimetallic catalysts for hydrocarbon reactions. Electrochemically, McNicol (2), and Moolhuysen and Jenssen (3) studied electrodeposited, supported platinum alloys as catalysts for electrooxidation of methanol in H_2SO_4 and found that certain platinum alloys, especially Pt-Sn, were significantly more active than platinum but lacked long term stability.

Very recently Jalan (4-6) successfully prepared and studied high surface area platinum-based metal alloys that were supported on carbon blacks. The oxygen reduction activities in concentrated phosphoric acid of some of these catalysts, e.g., platinum-vanadium alloys, were as much as an order of magnitude higher than platinum. It was also reported that at fuel cell conditions these alloys were more stable — lower rate of surface area loss and lower rate of activity loss — than platinum over about ten thousand hours. Although these results have since been verified by LBL (7), ERC (8), IGT (9) and UOP (10), there have been no reported evaluations of ternary alloys of platinum for oxygen reduction reactions.

Changes in surface structure, surface free energy, oxidation potential and metal-support interaction, are among the other factors that may alter the electrochemical characteristics of platinum-containing catalysts with alloying. These involve electronic (ligand effects) as well as geometric (ensemble effect) factors; an *a priori* determination of such effects is prohibitively complicated. Therefore, we chose to investigate, prepare and experimentally evaluate platinum alloys for use as oxygen reduction catalysts in phosphoric acid electrolyte.

Our initial efforts were directed at the preparation and characterization of known platinum alloys, such as Pt-Cr and Pt-V. From our characterization of these materials, and through searching in the patent literature (4-6), we discovered that as the platinum-platinum nearest neighbor distance decreased the electrochemical activity increased. A plot of specific activity for oxygen reduction at 900 mV versus the nearest neighbor distance for our alloy electrocatalysts, along with data from the patent literature, yielded a linear relationship, with the Pt-Cr electrocatalyst having the highest activity; this is explained in more detail in Section 7.0.

Based on this relationship, platinum alloys with smaller lattice constants should have high oxygen reduction activity. In **Figure 2-1**, the lattice parameter versus composition for various bulk alloys is presented. From this data, two approaches to forming platinum alloys with lower lattice parameters were apparent. In one approach, materials with lower lattice parameters such as Ni and Co were alloyed with platinum to form alloys with lower nearest neighbor distances than the Pt-Cr electrocatalyst. In the second, the recipes for forming particular alloy electrocatalysts were varied with the intent of changing the composition to form an electrocatalyst with a smaller nearest neighbor distance.

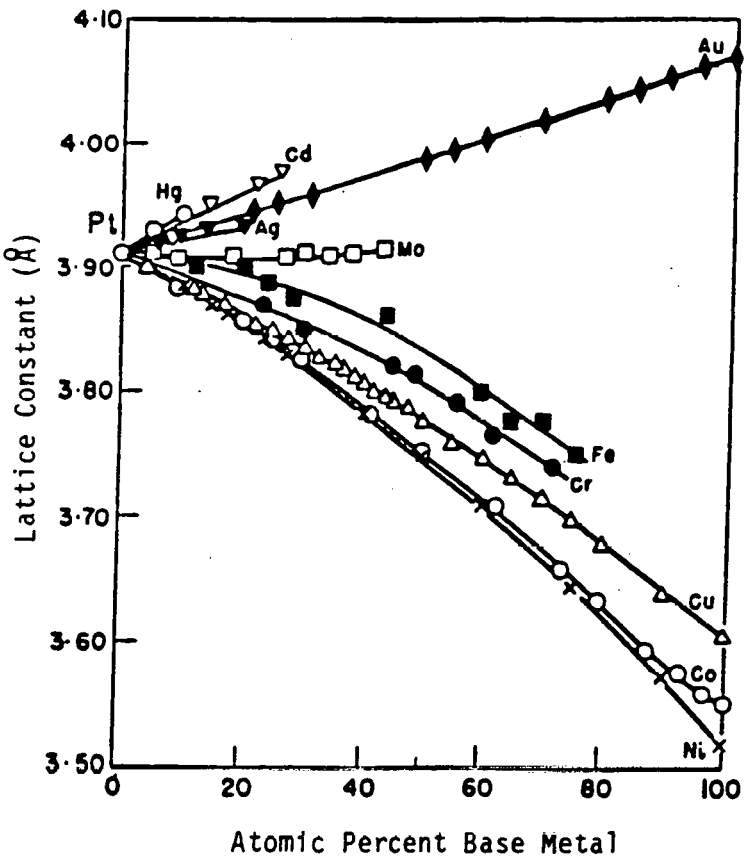

Figure 2-1. Variation of Lattice Constant with Composition of Various Platinum Alloys

2.2 NON-METALLIC ADDITIVES

The impetus for this work was the initial investigation of Jalan in the preparation of high surface area platinum carbide (11). It is known that when a high surface area platinum on high surface area carbon is heated to 900-1200°C, the resulting catalyst is more active than the starting materials. Jalan found that, if prior to the heat-treatment a small amount of carbon is deposited on Pt, the resulting catalyst is even better due to the formation of a high surface area platinum carbide (11, 12).

Another non-metallic additive considered promising for platinum-based electrocatalysts is sulfide, because sulfides of platinum are known to be conductive and have very high corrosion resistance compared to platinum alone (13). Additional work in this area, using non-metals such as boron and phosphorus, was completely exploratory.

2.3 REFERENCES FOR SECTION 2.0

1. Sinfelt, J.H., *Cat. Rev. — Sci. Eng.* **9**(1), 147-168 (1974).

2. McNichol, B.D., R.T. Short and A.G. Chapman, "Methanol Electro-oxidation Catalysts: Platinum Promoted by Tin," *J.C.S. Faraday I*, **72**, 2735 (1976).

3. Jenssen, M.M.P. and J. Moolhuysen, *Electrochemica Acta*, **21**, 869 (1976).

4. Jalan, V., "Noble Metal-Refractory Metal Alloy Catalysts and Methods for Making," US Patent No. 4,186,110 (1980).

5. Jalan, V., "Electrochemical Cell Electrodes Incorporating Noble Metal-Base Metal Alloy Catalysts," US Patent No. 4,192,907 (1980).

6. Jalan, V., "Noble Metal-Vanadium Alloy Catalysts and Method for Making," US Patent No. 4,202,934 (1980).

7. Ross, P.N., Jr., "Oxygen Reduction on Supported Pt Alloys and Intermetallic Compounds in Phosphoric Acid," Final Report for Contract RP 1200-5, Lawrence Berkeley Laboratory, Berkeley, CA (March 1980).

8. Energy Research Corp., Monthly Report No.4 for EPRI Contract RP 1200-1, Danbury, CT (June 1981).

9. Remick, R.J., "Stabilizing Platinum in PAFCs," Final Report for Contract DEN3-208, NASA CR-165606, IGT, Chicago, IL (July 1982).

10. Welsh, L.B., R.W. Leyerle, D.S. Scarlata and M.H. Vanek, "Development of Advanced Kocite Electrocatalysts for Phosphoric Acid Fuel Cells," Final Report for Contract DAAK 70-79-C-0173, UOP, Inc., Des Plaines, IL (January 1981).

11. Jalan, V., "Catalysts with Reduced Rate of Recrystallization and Methods for Making," US Patent No. 4,137,372 (1979).

12. Jalan, V., "High Activity Platinum Catalyst and Method for Making," US Patent 4,137,373 (1979).

13. Wold, A., in Platinum Group Metals and Compounds, (Advances in Chemistry Series: No.98), American Chemical Society (1971).

3.0 PREPARATION TECHNIQUES

3.1 INTRODUCTION

A number of different techniques were used in the preparation of platinum alloys evaluated during this program. In most cases the starting material was 10% Pt on a carbon support such as Vulcan XC-72, 2700°C heat-treated Vulcan XC-72 (HTV), or 2700°C heat-treated Black Pearls 2000 (HTBP). All these materials were platinized for Giner, Inc., by Johnson-Matthey, Inc. Several of the carbon supports were platinized in-house, evaluating new methods of depositing platinum on the carbon support. The platinized carbon support materials provided a high surface area starting material for the preparation of high surface area platinum alloys for use as cathodes in phosphoric acid fuel cells.

Only generalized procedures for alloy preparation will be given in this section; the specifics for each catalyst system will be presented in Chapter 5.

3.2 METAL OXIDE PRECIPITATION

The most common procedure used for the preparation of platinum alloys was the precipitation of base metal oxides onto a platinized support. This is shown conceptually in **Figure 3-1**, along with the associated chemical reactions. This procedure was used in the preparation of both binary and ternary alloys.

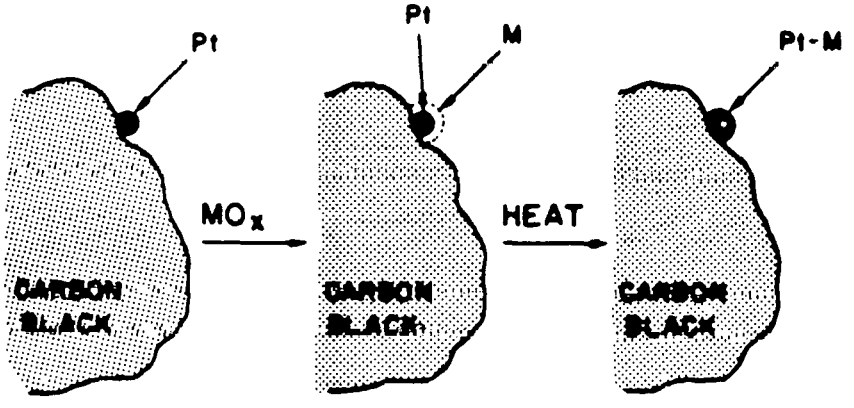

$$Pt/C + MO_x \longrightarrow Pt\text{-}M/C + CO_2$$

Figure 3-1. General Alloying Technique

In general, the appropriate amounts of base metal salts, typically nitrates, were added to a slurry of 10% Pt/carbon to yield a Pt:base metal ratio of 70:30 (binary alloys) or 70:15:15 (ternary alloys). The pH of the resulting slurry was slowly increased to a value of 11.0-11.5 to precipitate the base metals as metal oxides on the platinized support. The resulting slurry was filtered, and the recovered material was washed, dried and sieved. The dried material was then heat-treated for one hour at 900°C in an inert atmosphere to effect alloying.

3.3 CARBIDE FORMATION

A second method used in the formation of Pt alloys was carbide formation. This technique, described in US Patent 4,137,373, involved treatment of the catalyst powder with CO at low temperature (350-400°C) followed by 900°C heat-treatment under an inert atmosphere. The carbide formation procedure was used with 10% Pt/C, binary Pt alloys (to form ternary alloys) and ternary alloys (to form quarternary alloys).

3.4 AVOIDANCE OF METAL OXIDES

During the course of the program, evidence obtained from Lawrence Berkeley Laboratory suggested that base metal oxides might be present in our platinum alloy catalysts. The role of these metal oxides in the enhancement/degradation of alloy electrocatalyst activity under full cell conditions, relative to that of unalloyed platinum, is unknown. Therefore, various methods were evaluated to produce electrocatalysts having little or no metal oxide, as were methods for removal of metal oxides from electrocatalysts prepared by the standard method. These materials were referred to as "oxide-free" electrocatalysts, even though metal oxides may have been present. The generalized procedures used in the preparation of the oxide-free electrocatalysts were as follows:

3.4.1 Use of Organometallic Precursors

Using either 10% Pt/C or an unplatinized support, base metals and platinum were deposited on the support from a non-aqueous solution of an organometallic precursor. Subsequent to adsorption of the organometallic precursor onto the support, the support was dried and heat-treated under an inert atmosphere to decompose the organometallic and to promote alloy formation. Only binary alloys were prepared using this procedure.

3.4.2 Base Metal Sulfide Precipitation

This procedure was very similar to our standard method of preparation. However, instead of precipitating the base metals as oxides, they were precipitated as sulfides, followed by 900°C heat-treatment under hydrogen to decompose the sulfide and promote alloy formation.

3.4.3 Acid Leach

An alternative method for the preparation of an oxide-free electrocatalyst is to remove the metal oxides from electrocatalyst prepared by the standard method. Two methods were utilized. In the first, electrocatalyst powder was refluxed in boiling 18N H_2SO_4 for various lengths of time. The second procedure was similar, but 200°C, 100% H_3PO_4 was used instead of H_2SO_4. These experiments were conducted under a hydrogen atmosphere to prevent platinum dissolution.

4.0 EXPERIMENTAL PROCEDURES

4.1 INTRODUCTION

Subsequent to the preparation of electrocatalyst, the material was characterized by means of standard physical, chemical and electrochemical tests. Several of the tests were performed in-house, while outside vendors were used for specialized physical characterization testing.

4.2 PHYSICAL/CHEMICAL CHARACTERIZATION

Several different methods were used to determine the physical/chemical characteristics of the various electrocatalysts. For these tests, only electrocatalyst powder itself, prior to blending with polytetrafluoroethylene (PTFE) binder for electrode fabrication, was evaluated. All tests were performed by outside vendors.

4.2.1 Chemical Analysis

The composition of the electrocatalyst was verified by chemical analysis. This was done to ensure that the proper ratio of platinum to base metals was obtained during the preparation procedure.

4.2.2 X-Ray Diffraction (XRD)

Samples of electrocatalyst powder were also sent out for XRD analysis. This was used to confirm alloy formation from a change in the lattice parameter relative to that of platinum. In the range studied, the electrocatalysts exhibited reflections only from the (111), (200), and (220) family of planes indicating they all possess the face centered cubic (fcc) crystal structure (1). In fact, this was by design since we felt that changing the crystal structure from that of the platinum baseline electrocatalyst would unduly complicate our interpretation of the results.

Typical XRD data for supported platinum and platinum alloy electrocatalysts are presented in **Figure 4-1**. The first peak at ca. 2θ equal to 24° results from the carbon support material. The numbers in parentheses adjacent to each peak are the Miller indices for the crystallographic plane for the particular reflection. The spacing (d) between the various crystallographic planes may be calculated from the Bragg Law (2) for a first order reflection,

$$\lambda = 2d \sin\theta \qquad [4\text{-}1]$$

where λ is the wavelength of the incident X-ray in Å; d is the interplanar distance in Å; and θ is the angle of the incident X-rays. For our XRD analysis Cu K_α radiation with a wavelength of 1.540 Å was used. The interplanar distance calculated using the Bragg Law is given adjacent to each peak. (Note that the Bragg equation uses Å whereas the abscissa is given in terms of 2θ).

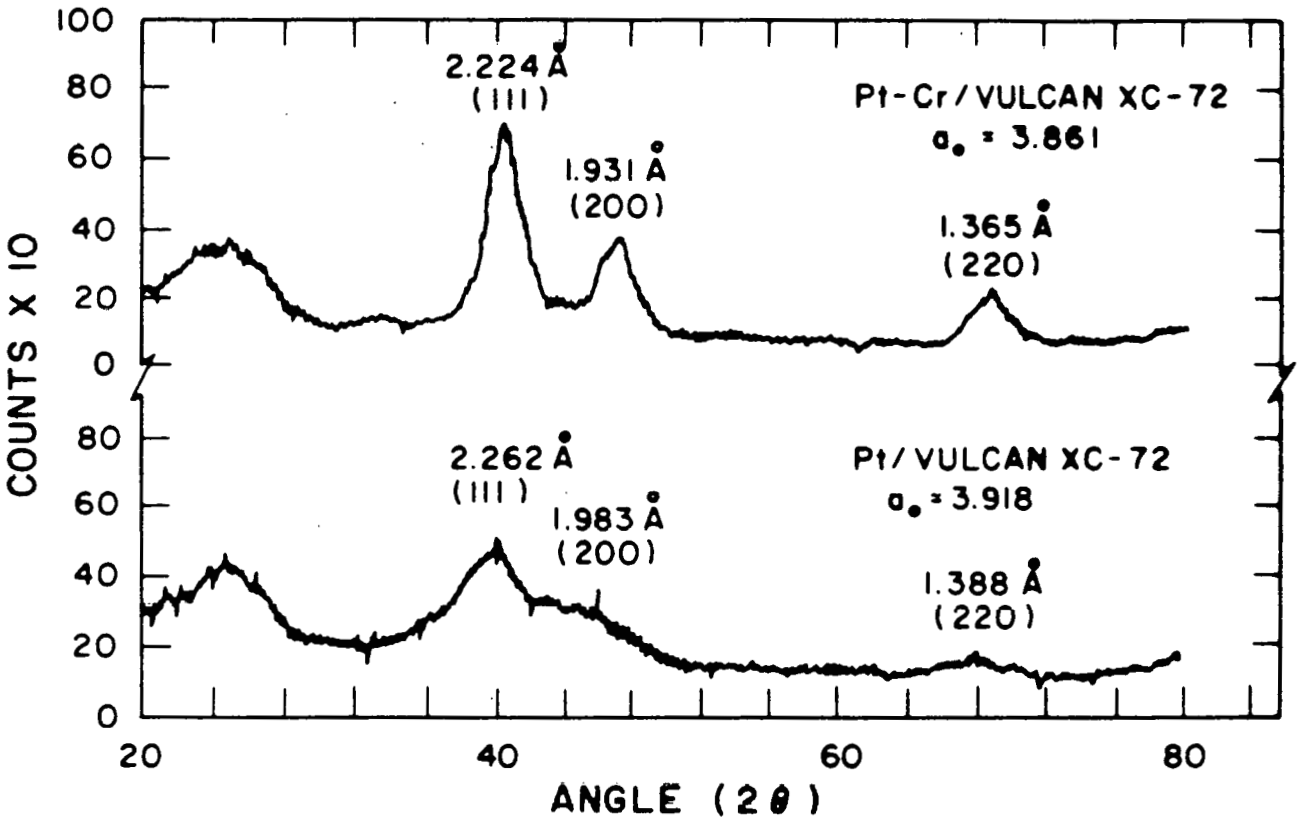

Figure 4-1. XRD Patterns of Pt/Vulcan and Pt-Cr/Vulcan XC-72 Electrocatalysts

For cubic systems (e.g., fcc), the lattice parameter may be calculated from the interplanar spacing (3),

$$a_o = d_{(hkl)} \sqrt{h^2 + k^2 + l^2} \qquad [4\text{-}2]$$

where a_o is the lattice parameter; h, k, l are the Miller indices for the given crystallographic planes; and $d_{(hkl)}$ is the interplanar spacing for the particular crystallographic plane.

The presence of single phase homogeneous alloys may be detected from the shape of the diffraction peak profile (4-6). Assymetric peak profiles are indicative of phase separation whereas symmetric peak profiles are indicative of the presence of a homogeneous single phase.

XRD data may also be used to determine the particle size of the alloy electrocatalyst. Small crystallites of 1000 Å diameter and less contribute to line broadening of the XRD peaks. The particle size, D, may be related to the XRD peak broadening by the Scherrer equation (7)

$$D = \frac{0.9\lambda}{B_C \cos\theta} \qquad [4\text{-}3]$$

$$B_C = (B_m^2 - B_S^2)^{\frac{1}{2}} \qquad [4\text{-}4]$$

where λ is the wavelength of the incident radiation, θ is the Bragg angle for the reflected peak, B_C is the peak broadening due to crystallite size, B_S is the peak broadening due to factors other than the crystallite size, and B_m is the measured peak broadening.

Enhanced activity and stability of platinum alloy catalysts were reported by Jalan (8-11) but no mechanisms relating the activity or stability to the structure were presented. The structure of a catalyst has long been considered to play an important role in determining the catalyst properties. In the field of alloy catalyst development much speculation regarding increased stability of intermetallic compounds resulting from their ordered structure has been given. More specifically, increased activity and stability of platinum alloy electrocatalysts for oxygen reduction in acid has been attributed to intermetallic formation with the resultant modification of the platinum electronic properties via ligand effects (12, 13). The most promising systems were Pt-V, Pt-Ta, Pt-Zr, and Pt-Hf. All were reported to form intermetallics with an ordered fcc structure of the $AuCu_3$ type.

We have examined our catalyst XRD data for possible intermetallic formation. In **Figure 4-2**, the structures of a 25/75 Au-Cu solid solution alloy and the $AuCu_3$ intermetallic are presented. For the completely disordered substitutional solid solution in Figure 4-2a, the probability that a particular site is occupied by a gold atom is 1/4 and by a copper atom is 3/4. These probabilities are the same for every site and we may regard each site to be occupied by a statistically average gold-copper atom. In the case of the intermetallic pictured in Figure 4-2b, the corner sites are occupied by

gold atoms and the face center sites are occupied by copper atoms. In both cases the ratio of copper to gold atoms is 3 to 1. Both structures are cubic and have nearly the same lattice parameter. Nevertheless, there will be differences in the X-ray diffraction patterns of these two structures.

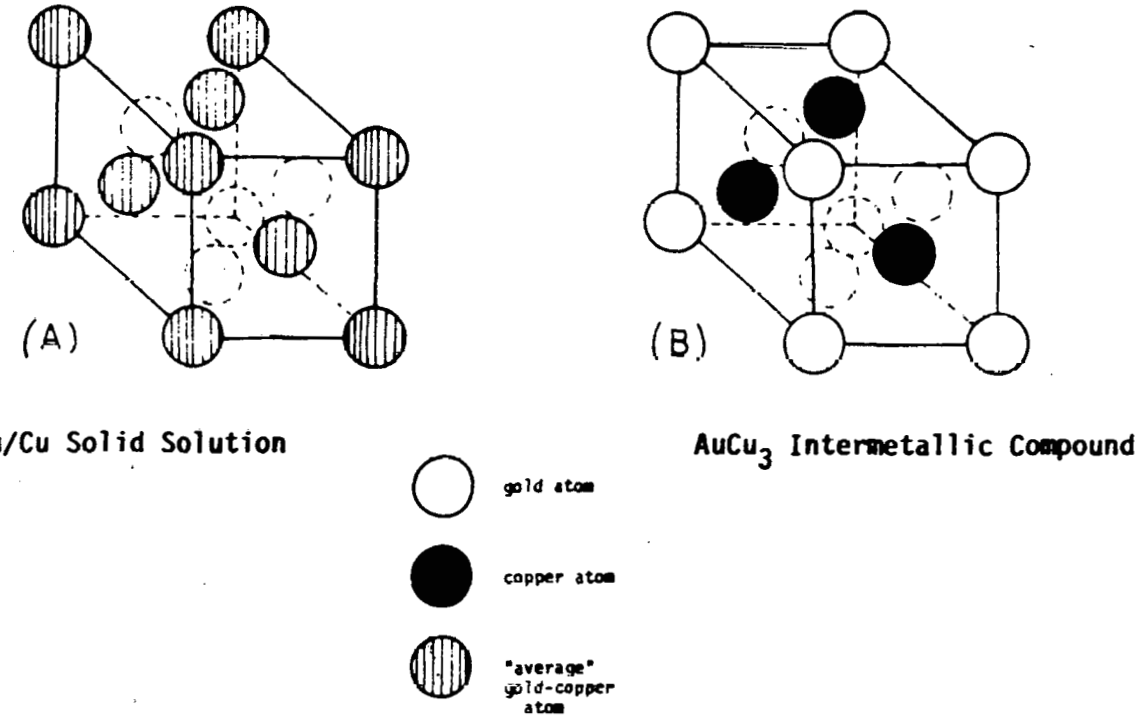

Figure 4-2. Gold-Copper Solid Solution and Intermetallic

The intensity of an XRD reflection is proportional to the square of the structure factor, F. The relative structure factor may be calculated from the atomic scattering factor, f, of the various atoms in the unit cell. The atomic scattering factor is a function of the incident x-ray wavelength and the angle of the diffracted beam and may be found tabulated for various atoms versus $(\sin\theta)/\lambda$ (14). For the structure in Figure 4-2a, it may be shown (15) that the peak intensities from crystal planes given by all even or all odd Miller indices (i.e., khl unmixed) are proportional to:

$$I \cdot F^2 = (f_{Au} + 3f_{Cu})^2 \qquad [4\text{-}5]$$

and for crystal planes given by a mix of even and odd Miller indices (i.e., hkl mixed) the peak intensities are proportional to:

$$I\text{-}F^2 = 0 \qquad [4\text{-}6]$$

These equations are valid for any fcc material with the appropriate scattering factors inserted. For example, the peak intensities for platinum, with an fcc structure, from planes of unmixed hkl:

$$I\text{-}F^2 = 16\ f_{Pt}^2 \qquad [4\text{-}7]$$

and for hkl mixed:

$$I\text{-}F^2 = 0 \qquad [4\text{-}8]$$

For the intermetallic compound pictured in Figure 4-2b, Equation [4-5] remains unchanged but for hkl mixed the intensities are proportional to:

$$I\text{-}F^2 = (f_{Au} - f_{Cu})^2 \qquad [4\text{-}9]$$

The diffraction lines from the unmixed hkl planes exist in both the ordered and disordered alloy at the same positions with the same intensities and are called fundamental lines. However, in the ordered alloy, extra lines, called superlattice lines, from the mixed hkl planes are apparent and their presence is direct evidence of intermetallic formation.

Since the intensities of the superlattice lines result from a difference in atomic scattering factors, they will necessarily be lower in intensity than the fundamental lines. For example, the ratio of the superlattice line intensity, I_s, to the fundamental line intensity, I_f, may be approximated by:

$$\frac{I_s}{I_f} \cdot \frac{F_s^2}{F_f^2} = \frac{(f_{Au} - f_{Cu})^2}{(f_{Au} + 3f_{Cu})^2} \qquad [4\text{-}10]$$

where f_{Au} and f_{Cu} are the atomic scattering factors for gold and copper, respectively. The atomic scattering factor is a function of $\sin\theta$ and λ, but at $(\sin\theta)/\lambda = 0$, the atomic scattering factors are equal to the atomic numbers of the respective atoms. Hence, an approximation of the relative intensities of the fundamental and superlattice lines may be obtained from Equation [4-10].

4.2.3 Transmission Electron Microscopy (TEM)

All of the supported electrocatalysts were characterized via TEM to determine their degree and uniformity of dispersion. Assuming spherical catalyst morphology, the specific surface areas of the supported electrocatalysts may be calculated from

$$S = \frac{6 \times 10^4}{\rho D} \qquad [4\text{-}11]$$

where S is the specific surface area in m^2/g; ρ is the density of platinum, 21.4 g/cm^3; and D is the average particle diameter in Angstroms. The density of platinum was used in all calculations and we assumed the density of the alloys is roughly the same as platinum (in platinum rich alloys, the "error" will be less than 20%). In most cases, good agreement was observed between specific surface areas determined from hydrogen adsorption (Section 4.3.1) and TEM data.

4.2.4 Energy Dispersive Analysis by X-Rays (EDAX)

Select electrocatalyst powders were analyzed for elemental composition by EDAX. In this analysis, a single alloy particle was analyzed to verify all the components were present in the particle.

4.2.5 Electron Spectroscopy for Chemical Analysis (ESCA)

The standard Giner, Inc., alloy electrocatalyst preparation technique involves the deposition of base metal oxides onto a platinized support, followed by heat-treatment to effect alloy formation. ESCA was used in an attempt to determine the chemical state of the metal components of select electrocatalysts. The objective was to determine whether metals, metal oxides, or combinations of both were present in the electrocatalyst.

4.3 ELECTROCHEMICAL CHARACTERIZATION

Gas diffusion electrodes were fabricated from the various alloy electrocatalysts for electrochemical evaluation. Electrodes typically contained precious metal loadings of 0.5 mg/cm^2 with 40% PTFE binder, and were sintered at 345°C. The electrodes were supported on wetproofed carbon fiber paper (Stackpole Corporation, Type PC-206). To insure complete wetting, electrodes used in cyclic voltammetry contained only 10% PTFE.

4.3.1 Cyclic Voltammetry

All electrocatalysts were evaluated by means of cyclic voltammetry to determine the electrochemical surface area from the hydrogen adsorption region in the cyclic voltammogram. These measurements were made in 50% H_3PO_4 at 25°C.

The sample (a 1 cm^2 disk cut from a large electrode) was soaked overnight in an isopropanol-H_3PO_4 mixture, then rinsed in pure electrolyte prior to entry into the electrochemical cell. The potential of the sample was recorded versus the dynamic hydrogen electrode (DHE), which has a negligible (<1 mV) polarization versus the reversible hydrogen electrode. The electrode was cycled three times between +0.050 and +1.400 V at 50 mV/sec. The scan rate was then lowered to 10 mV/sec and a complete cycle recorded. The area under the hydrogen adsorption peak was integrated to yield the cathodic charge for the deposition of hydrogen. This value was then used to calculate the specific surface area of the electrocatalyst, using the commonly accepted value of 210 $\mu c/cm^2$ (16) to convert from hydrogen cathodic charge to specific surface area.

4.3.2 Floating Electrode Half-Cell Testing

The electrochemical activity of the electrocatalysts was evaluated using the floating electrode half-cell apparatus (17), shown in **Figure 4-3**. These measurements were conducted in 200°C, 100% H_3PO_4 with the reactant gas (either oxygen or air) presaturated in water at 60°C prior to entry into the cell. All voltages were measured with respect to a DHE reference electrode; the voltages were corrected for cell iR drop by means of a current interruption technique. As with the cyclic voltammetry experiments, a 1 cm^2 disk electrode was used.

4.3.3 Full Cell Testing

All full cell testing was performed using sub-scale laboratory size PAFC hardware; active electrode area was 25 cm^2. All builds used 10% Pt/Vulcan XC-72 as the anode electrocatalyst with a 6 mil SiC matrix. Standard atmospheric test conditions were 200 mA/cm^2, 190°C, 50% utilization of air (O_2) and 80% utilization of the anode gas (H_2) which was presaturated at 72°C to maintain 100% H_3PO_4. Standard full cell pressurized test conditions were identical except for operation at 267 mA/cm^2 and 70 psia. A number of pressurized full cell tests were also run at 200 mA/cm^2 and 70 psig. Stability testing was performed for times ranging from several hundred up to 10,000 hours in length. Cell voltages were corrected for iR losses by means of a current interruption technique.

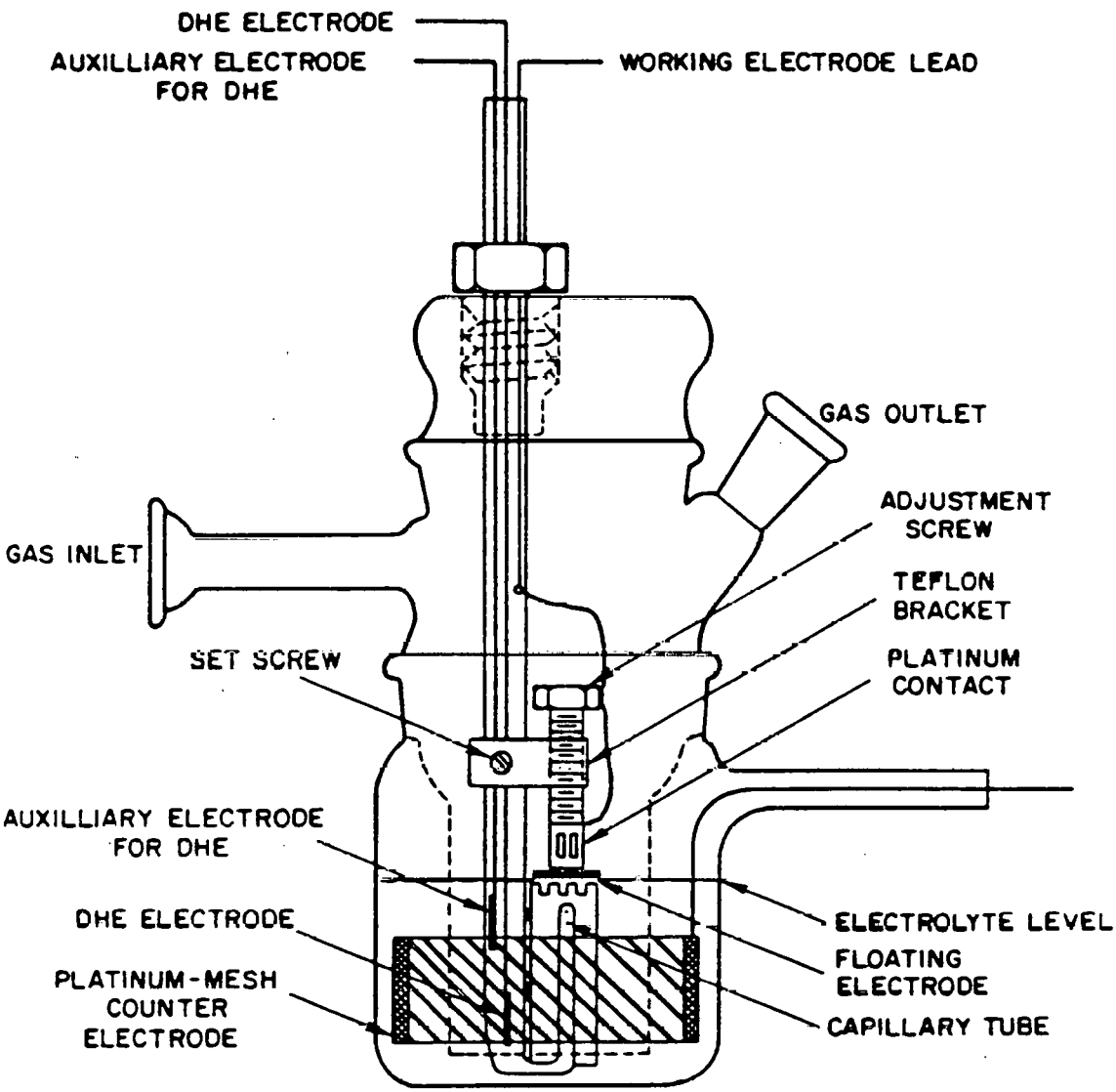

Figure 4-3. Floating Electrode Half-Cell Apparatus

4.4 REFERENCES FOR SECTION 4.0

1. Reed-Hill, R., Physical Metallurgy Principles, 2nd ed., Van Nostrand Co., NY, p. 891 (1973).

2. *Ibid.*, p. 40.

3. *Ibid.*, p. 47.

4. Cormack, D., et al., *J. Catalysis*, **32**, 494 (1972).

5. Moss, R. and H. Gibbers. *J. Catalysis*, **24**, 48 (1972).

6. Moss, R., et al., *J. Catalysis*, **16**, 117 (1970).

7. Cullity, B.D., Elements of X-Ray Diffraction, Addison-Wesley, Reading, MA, p. 284 (1978).

8. Jalan, V., "Noble Metal-Vanadium Alloy Catalyst and Method for Making," US Patent No. 4,202,934 (1980).

9. Jalan, V., US Patent No. 4,186,110 (January 29, 1980).

10. Jalan, V., US Patent No. 4,192,907 (March 11, 1980).

11. Jalan, V., "Activity Enhancement of Platinum by Alloying with Base Metals," Abstract No. 350, Electrochemical Society Meeting, Montréal, Canada (May 9-14, 1982).

12. Ross, P.N., National Fuel Cell Seminar, San Diego, CA (July 14-16, 1980).

13. Ross, P.N., EPRI Final Report for Contract RP 1200-5 (March 1980).

14. Cullity, B.D., "Appendix 12" in Elements of X-Ray Diffraction, Addison-Wesley, Reading, MA (1978).

15. *Ibid.*, pp.384-385.

16. Bett, J., K. Kinoshita, K. Routsis and P. Stonehart. *J. Catalysis*, **29**, 160 (1973).

17. Giner, J. and S. Smith, *Electrochem. Technol.*, **5**, 61 (1967).

5.0 STUDIES ON INDIVIDUAL SYSTEMS

5.1 INTRODUCTION

During the course of the program, a total of 81 electrocatalysts were either procured commercially or, for the majority of the electrocatalysts, prepared in-house. These materials were all supported on various carbon blacks and included platinum, platinum binary alloys and their associated carbides, and platinum ternary alloys and their associated carbides. In addition to varying the composition of the alloying components, various electrocatalyst supports, including graphitized materials for improved corrosion resistance, were evaluated to determine their effect on electrocatalyst performance/stability, especially for fuel cell operation under pressurized conditions. This chapter summarizes the preparation procedures utilized and the results obtained during the characterization of the individual systems.

5.2 PLATINUM AND CARBIDES

Task I: Materials Selection

A commercially available platinum supported on Vulcan XC-72 was selected as the baseline catalyst material as well as the precursor for the advanced catalysts. For this purpose, 5% Pt/Vulcan and 10% Pt/Vulcan were obtained from Johnson-Matthey; in-house platinization techniques were used only as required.

The use of pressurized fuel cell operating conditions places an increased stress on the carbon black electrocatalyst support, resulting in increased corrosion of the support. Therefore, the use of corrosion-resistant supports was examined. These included Shawinigan Acetylene Black (SAB), 2700°C heat-treated Vulcan XC-72 (HTV) and 2700°C heat-treated Black Pearls 2000 (HTBP). Vulcan XC-72 and Black Pearls 2000 were obtained from Cabot Corp. (Billerica, MA) and subjected to a 2700°C heat-treatment, in an inert atmosphere, by Midland Research, Midland, MI.

Task II: Catalyst Preparation

The platinized supports were either purchased directly from or platinized for Giner, Inc. by Johnson-Matthey. "Pt carbide"/Vulcan XC-72 was prepared as described by Jalan (1, 2) as follows: A ten-gram sample of the 10% Pt on Vulcan was first exposed to carbon monoxide at

350-400°C for approximately 20 minutes. The sample was then heated under nitrogen at 900°C for one hour, followed by an additional twenty minutes at 350°C in carbon monoxide. An identical procedure was used for the preparation of Pt-C/SAB.

Task III: Characterization

The above electrocatalysts were fabricated into gas diffusion electrodes and evaluated for surface area using electrochemical hydrogen adsorption. Results are summarized in **Table 5-I**. The 5% Pt/Vulcan electrocatalyst was not characterized for surface area or by XRD analysis, as it was felt that too much material was required to yield an electrode with a Pt loading of 0.5 mg/cm².

TABLE 5-I

PROPERTIES OF PLATINIZED ELECTROCATALYST SUPPORTS

Electrocatalyst	Lattice Parameter (Å)	Surface Area (m^2/g) EC	TEM	Diameter (Å)
5% Pt/Vulcan	——	—	—	—
10% Pt/Vulcan	3.918	139/143	153	19
Pt/SAB	3.958	69	—	—
Pt/HTV	——	79	122	23
Pt-C/Vulcan	3.909	87	62	45
Pt-C/SAB	——	76	76	37

The supported electrocatalysts were characterized via TEM to determine their degree and uniformity of dispersion; most of the materials were uniform. Assuming spherical catalyst morphology, the specific surface areas of the supported platinum electrocatalysts may be calculated from

$$S = \frac{6 \times 10^4}{\rho D} \qquad [5\text{-}1]$$

where S is the specific surface area in m^2/g; ρ is the density of platinum (21.4 g/cm^3); and D is the average particle diameter in Å. The average particle diameters observed in the TEMs and specific surface areas calculated from Equation [5-1] are also tabulated in Table 5-I. We have used the density of platinum for all calculations, even when calculating specific surface areas of platinum alloys, and have assumed that the density of the alloys is roughly the same as platinum.

The diameters of the carbides were approximately double those of the platinized supports; this was due to sintering which occurred during the 900°C heat-treatment step in carbide formation.

Several of these materials were also characterized by XRD. Calculated lattice parameters are summarized in Table 5-I. The lattice parameter for the Pt/Vulcan electrocatalyst, 3.918 Å, is in reasonable agreement with the 3.923 Å value for bulk platinum. The change in lattice parameter of Pt-C/Vulcan to 3.909 Å is indicative of platinum carbide alloy formation. Although platinum carbide has not yet been observed in the bulk, its existence has been reported in thin film form (3, 4).

Task IV: Electrochemical Evaluation

All of the platinum and platinum carbide electrocatalysts were evaluated for cathode activity in the floating electrode half-cell apparatus. Results are summarized in **Table 5-II**. The highest performance was observed for the carbided electrocatalysts. Oxygen gains, listed in the last column of Table 5-II are a qualitative measure of the integrity of the electrode structure. The theoretical difference between oxygen and air performance, given by

$$E = \text{Tafel Slope} \times \log[O_2 \text{ partial pressure ratio}] \qquad [5\text{-}2]$$

is 61 mV. Values higher than this are typically due to partial flooding in a poor electrode structure.

TABLE 5-II

HALF-CELL RESULTS, PLATINIZED SUPPORTS

Electrocatalyst	iR-Free Performance* at 200 mA/cm² (mV)		
	O_2	Air	Gain
5% Pt/Vulcan	760	700	60
10% Pt/Vulcan	745	685	60
Pt/SAB	745	678	67
Pt/HTV	725	638	87
Pt/HTBP 2000	746	663	83
Pt-C/Vulcan	760	690	70
Pt-C/SAB	760	690	70

***Test Conditions:** Floating Electrode Half-Cell, 100% H_3PO_4 at 200°C

The 10% Pt/Vulcan electrocatalyst was evaluated under full cell operating conditions. Testing was conducted at the standard atmospheric pressure test conditions of 200 mA/cm², 190°C and 50% utilization of air/oxygen and 80% utilization of the anode gas (H_2) which was presaturated at 72°C to maintain 100% H_3PO_4. Results of this test are summarized in **Figure 5-1**.

5.3 ALLOYS WITH VANADIUM, CHROMIUM AND CERIUM

Task I: Materials Selection

After a review of the patent literature, Pt-V, Pt-Cr and their associated carbides were selected for preparation and evaluation with a goal of establishing a database to establish selection criteria for future candidate electrocatalysts. Pt-Ce and Pt-Ce-C were also selected for inclusion in this group.

Task II: Catalyst Preparation

The Pt-V/Vulcan alloy electrocatalyst was prepared according to a procedure published by Jalan (5). Summarizing this procedure, V_2O_5 was dissolved in basic solution, allowed to react with hydrogen peroxide and sodium dithionite and finally combined with a Pt/Vulcan slurry. After one hour the slurry was filtered, dried and subsequently heat-treated for one hour at 930°C in a nitrogen atmosphere to form a Pt-V/Vulcan alloy. The Pt-V-C/Vulcan XC-72 ternary alloy catalyst was produced by submitting the Pt-V catalyst to the CO treatment described in Section 5.2.

A procedure described by Landsman (6) was used to prepare the Pt–Cr/Vulcan alloy electrocatalyst: 10% Pt/Vulcan was dispersed in a dilute ammonium hydroxide solution, to which was added ammonium chromate. The resulting slurry was acidified with HCl, filtered, dried and heat-treated at 930°C for one hour in a nitrogen atmosphere for alloy formation.

The Pt-Ce/Vulcan alloy electrocatalyst was prepared starting with an acidic slurry of Pt/Vulcan to which was added $(NH_4)_2Ce(NO_3)_6$. The pH was adjusted to 6 to precipitate cerium hydroxide. The resulting slurry was then filtered and dried. One half of the material was subjected to the standard, one-hour heat-treatment while the other half was carbided to form Pt-Ce-C/Vulcan.

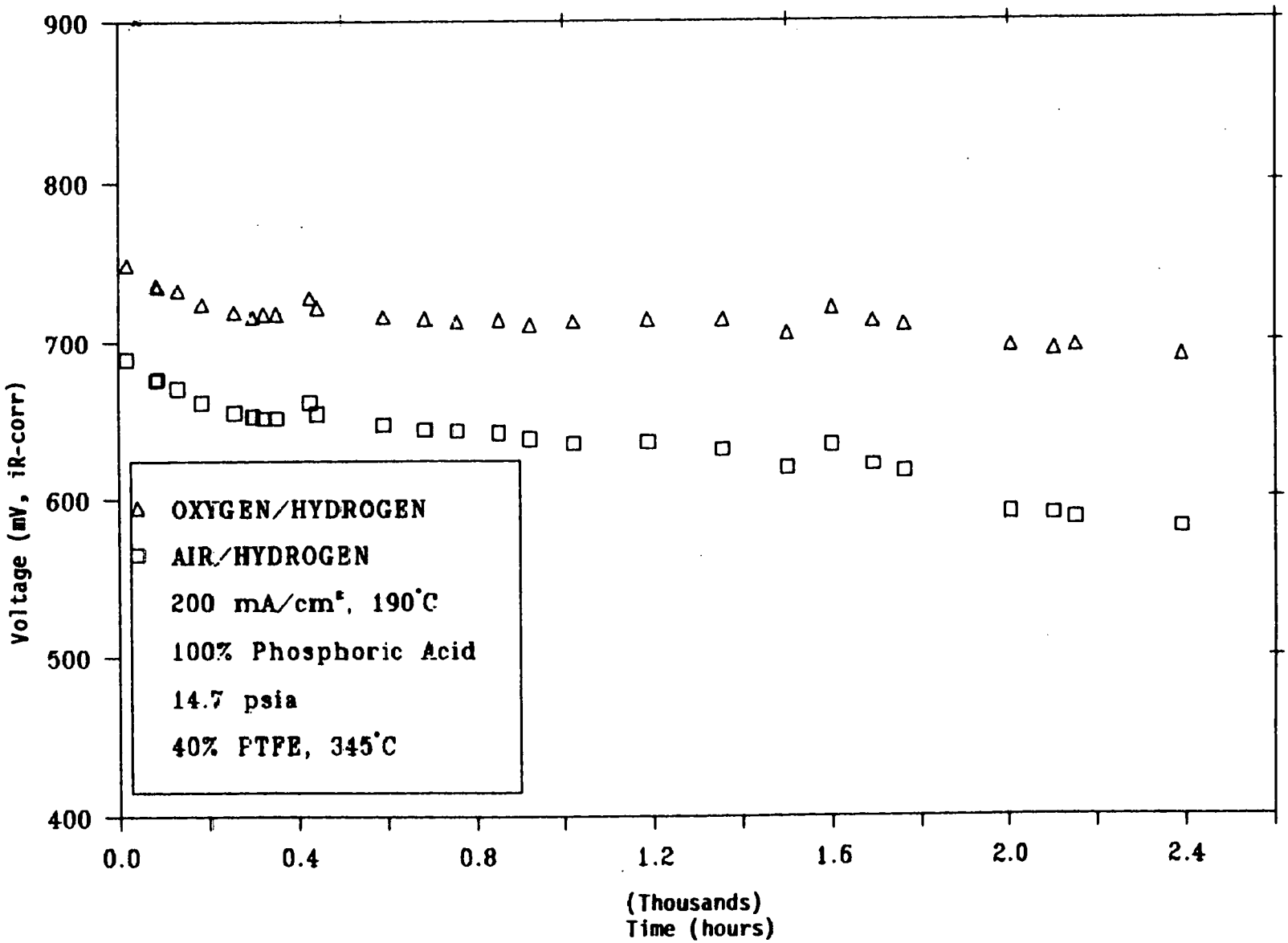

Figure 5-1. Life Performance of Fuel Cells Containing Pt/Vulcan

This procedure was also used to prepare two Pt-Cr-Ce/Vulcan alloy catalysts. Using the above method, cerium hydroxide was precipitated onto the Pt-Cr/Vulcan catalyst. The first catalyst was prepared by heating this material under hydrogen at 600°C for one half-hour to facilitate alloying, while a second catalyst was prepared from this material by alloying under nitrogen at 900°C for one hour.

Similar procedures were used to prepare the Pt-Cr-Ce electrocatalyst on SAB and HTV supports.

Task III: Characterization

The supported platinum alloy electrocatalysts were characterized by XRD, TEM, EDAX and CV (cyclic voltammetry). Representative characterization data are summarized in **Table 5-III**. The particle sizes of the alloy electrocatalysts were typically 38-90 Å in diameter, or 40-84 m^2/g specific surface area (measured by CV). The decrease in surface area of the alloy electrocatalysts, relative to that of 10% Pt/Vulcan (Table 5-I) is attributed to the 900°C heat treatment used in their preparation. The Pt-V and Pt-V-C electrocatalysts exhibited considerably larger particle sizes and were not considered to be good electrocatalyst preparations.

TABLE 5-III

PROPERTIES OF V, Cr, Ce ALLOYS AND CARBIDES

Electrocatalyst	Lattice Parameter (Å)	Surface Area (m^2/g) EC	TEM	Diameter (Å)
Pt-V	3.901	40	34	83
Pt-V-C	3.902	47	31	90
Pt-Cr	3.863	73	74	38
Pt-Cr-C	3.867	84	68	41
Pt-Ce	*	78	58	48
Pt-Ce-C	*	63	—	—
Pt-Cr-Ce(H_2)	3.881	84	65	43
Pt-Cr-Ce(N_2)	3.865	69	61	46
Pt-Cr-Ce/SAB	3.890	55	—	—
Pt-Cr-Ce/HTV	3.903	41	—	—

*Phase separation

Most of the electrocatalysts were characterized by means of TEM; uniform dispersions were observed.

The XRD patterns of the alloy electrocatalysts were obtained and analyzed. From this data, it was concluded that we have indeed formed platinum alloys and all the alloys possessed the fcc crystal structure. Additional information regarding phase homogeneity, phase structure, and crystallite size have also been extracted from the XRD measurements.

(i) Phase Homogeneity and Structure

The presence of single phase homogeneous alloys may be detected from the shape of the diffraction peak profiles (7, 8, 9). Asymmetric peak profiles are indicative of phase separation whereas symmetric peak profiles are indicative of the presence of a homogeneous single phase. All the diffraction peaks (i.e., for d_{111}, d_{200}, and d_{220}) for all the alloy electrocatalysts except Pt-Ce and Pt-Ce-C were symmetrical and suggest single phase formation. For Pt-Ce and Pt-Ce-C, asymmetric diffraction peak profiles were observed and are indicative of phase separation and non-homogeneity.

For some of the alloy systems we have investigated, the existence of both the solid solution and the $AuCu_3$ type intermetallic have been reported; Pt_3Cr (10), Pt_3Al (11), and Pt_3V (12). For the platinum-chromium system, using Equation [4-10] with the atomic numbers of platinum and chromium, the approximate intensity of the intermetallic superlattice lines should be 4% of the intensity of the fundamental lines. Our preliminary observations do not detect superlattice lines in the X-ray diffraction pattern of the Pt-Cr electrocatalyst or any of the other electrocatalysts, indicating that the platinum alloys are all solid solutions. However, due to the low content of the metal (10% metal -90% carbon), the small particle size, and the possibility that the alloy may consist of both solid solution and intermetallic, the X-ray diffraction patterns are diffuse and consequently the detection of superlattice lines is difficult.

Although Ross (13, 14) reported the formation of intermetallics with an fcc structure of the $AuCu_3$ type in his investigation, he only reports the lattice parameters of his materials and did not mention the detection of superlattice lines. Since the actual diffraction patterns were not presented, it is not possible to ascertain whether intermetallics were indeed formed. Moreover, the intermetallics Pt_5Ta, Pt_4Zr, and Pt_4Hf which were reportedly formed do not belong to the $AuCu_3$ class. Consequently, we believe that the rationale and presumed benefits of intermetallic formation via increased stability due to long range ordering are yet to be demonstrated.

Furthermore, the formation of a specific type of intermetallic (e.g., the $AuCu_3$ type) is strongly dependent on the preparation and processing history. For example, Meschter and Worrell (15) have extensively investigated the thermodynamics and stability of various phases in the Pt-Ti alloy system. Citing their work and the work of others, they conclude that the Pt_3Ti intermetallic is stable and has the fcc $AuCu_3$ type structure only above 1200°C. However, in the 900-1300°C temperature range, the Pt_3Ti intermetallic has the hcp $TiNi_3$ type structure (16). Finally, no ordered Pt_3Ti phases are observed in the case of alloys heat treated at 1000°C where the equilibration times are less than 48 hours (17). Because of our alloying temperature, 900°C, and our relatively short equilibration time, one hour, the fact that our platinum alloys all formed fcc solid solutions was consistent with the work of Meschter and Worrell.

As will be discussed in Chapter 7, we have reported that the lattice constants and nearest-neighbor distances decreased as the alloy electrocatalyst activity increased. This correlation between catalyst activity and platinum-platinum nearest neighbor distance was rationalized in terms of a dual site mechanism for the oxygen reduction reaction (18). As is evident from the (100) crystal plane of the Pt_3Cr fcc $AuCu_3$-type intermetallic and the 75-25 Pt-Cr solid solution shown in **Figure 5-2**, large changes in the platinum-platinum nearest-neighbor distances would result from intermetallic formation. The electrochemical evaluation of a well characterized intermetallic would be of great interest to researchers in the field and should provide further confirmation of our correlation to predict catalytic activity for platinum alloys.

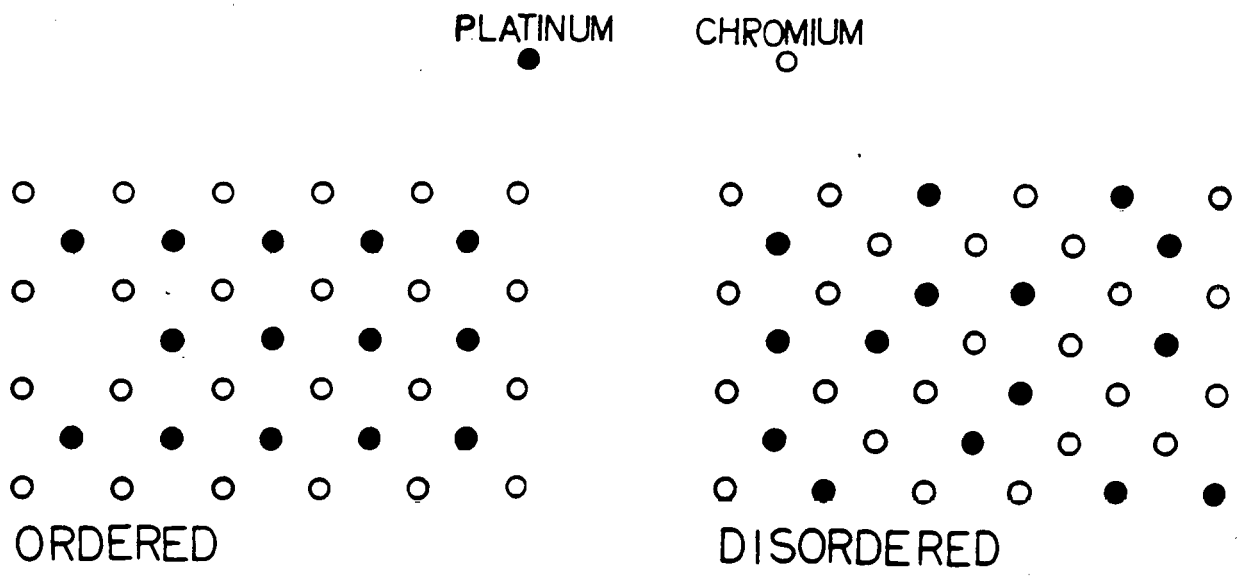

Figure 5-2. Pt_3Cr Intermetallic (Ordered) and 75-25 Pt-Cr Solid Solution (Disordered)

Task IV: Electrochemical Characterization

The half-cell oxygen reduction activity of the alloy electrocatalysts was determined and, along with the platinum standard for comparison, is summarized in **Table 5-IV**. The platinum loading of a typical electrode was determined from chemical analysis to be 0.42 mg of platinum per cm^2. This loading was then used to calculate the mass activity (mA/mg Pt) at 900 mV for oxygen reduction. Using the mass activity, specific surface area, and nearest-neighbor distance data a plot of relative specific activity versus nearest-neighbor distance was prepared and is shown in **Figure 5-3**. The Pt-V and Pt-V-C electrocatalysts are not included in Figure 5-3 because of their non-uniform dispersion, while the Pt-Ce and Pt-Ce-C electrocatalysts are not included because the XRD analysis indicated that these preparations did not form homogeneous solid solutions, and consequently a meaningful lattice parameter could not be derived. For the other alloy electrocatalysts, the data fits the correlation of increasing activity with decreasing nearest-neighbor distance.

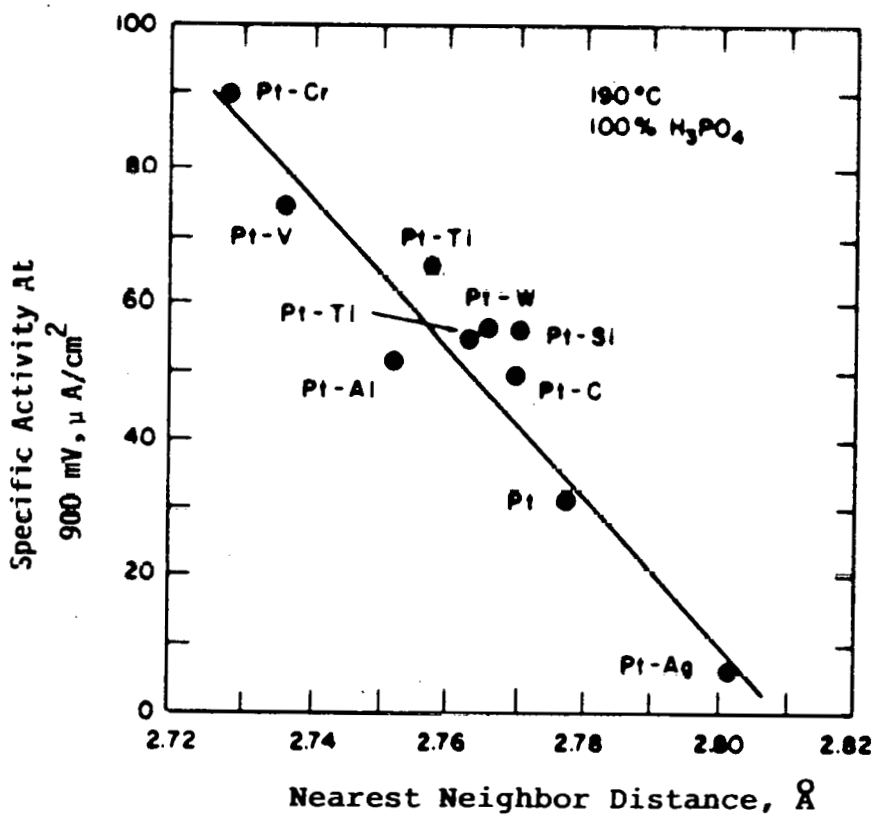

Figure 5-3. Specific O_2 Reduction Activity

TABLE 5-IV

HALF-CELL REDUCTION ACTIVITY

Electrocatalyst	iR-Free Performance* at 200 mA/cm² (mV)	
	O_2	Air
Pt-V	770	705
Pt-V-C	770	695
Pt-Cr	785	735
Pt-Cr-C	795	740
Pt-Ce	770	695
Pt-Ce-C	765	710
Pt-Cr-Ce(H_2)	790	735
Pt-Cr-Ce-N_2)	805	735
Pt-Cr-Ce/SAB	754	697
Pt-Cr-Ce/HTV	744	665
Pt	745	685

***Test Conditions**: Floating Electrode Half-Cell, 100% H_3PO_4, 200°C

Task V: Stability Testing

Complete subscale (2" x 2" active area) fuel cell testing of the Pt-Cr-Ce and Pt-Cr-C cathode electrocatalysts was conducted. These cells were operated at 190°C, 200 mA/cm², atmospheric pressure using 100% H_3PO_4 on hydrogen (80% utilization) and air (50% utilization) and were each run in excess of 1200 hour continuous operation. In **Figures 5-4** and **5-5**, the variation of the open circuit voltage and the iR-free voltage at 200 and 325 mA/cm² with time on air and oxygen are presented. Both cells exhibited similar stability with the performance of Pt-Cr-C 5-10 mV higher than that of Pt-Cr-Ce. The performance decrease between the 21 and 1192 hour mark, at 10, 20, 100, 200 and 400 mA/cm² are tabulated in **Table 5-V**. Rather than exhibiting a constant voltage loss across the current range as one would expect if the activity decrease were due to electrocatalyst losses, we observed a minimum performance loss at 100 mA/cm² of 29 and 31 mV for the Pt-Cr-Ce and Pt-Cr-C electrocatalysts, respectively. At current densities greater than 100 mA/cm², the increasing performance loss, plus increasing oxygen gain, with increasing current density is attributed to electrode structure degradation. However, at current densities less than 100 mA/cm², the increasing performance loss and the decreasing open circuit potential with decreasing current density is indicative of increasing mixed potential.

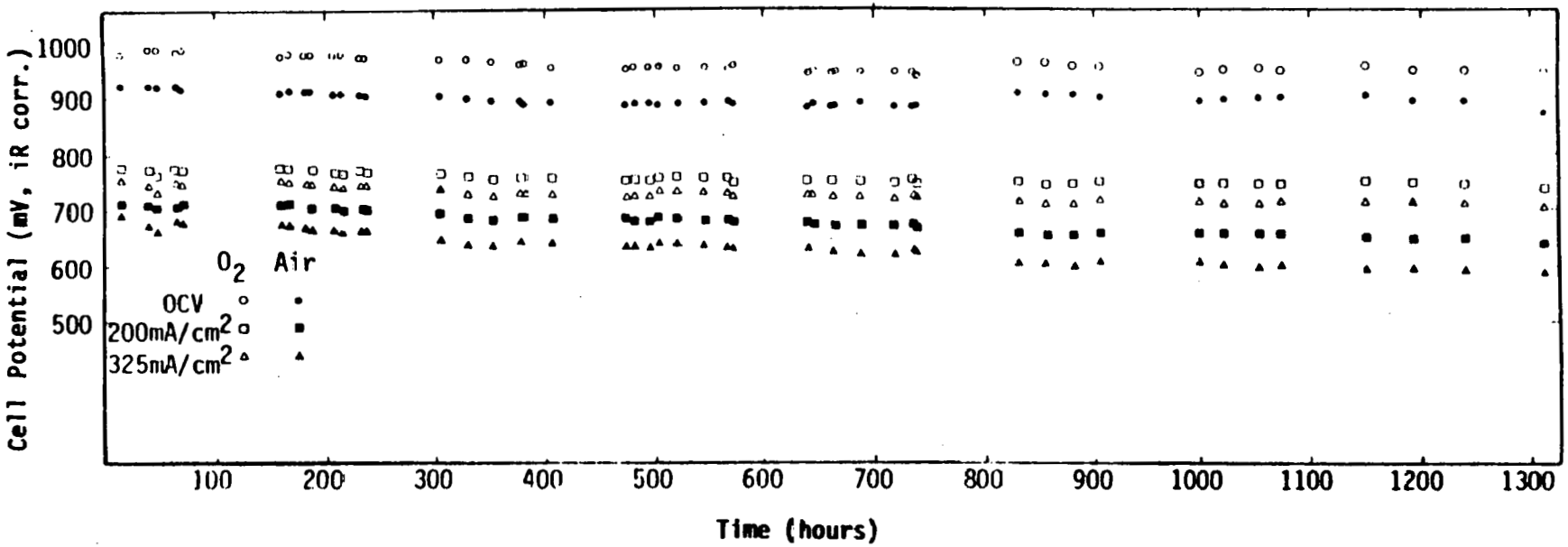

Figure 5-4. Voltage Stability of Fuel Cell Containing Pt-Cr-Ce Electrocatalyst at Open Circuit, 200 mA/cm² and 325 mA/cm² on Oxygen and Air at 190°C

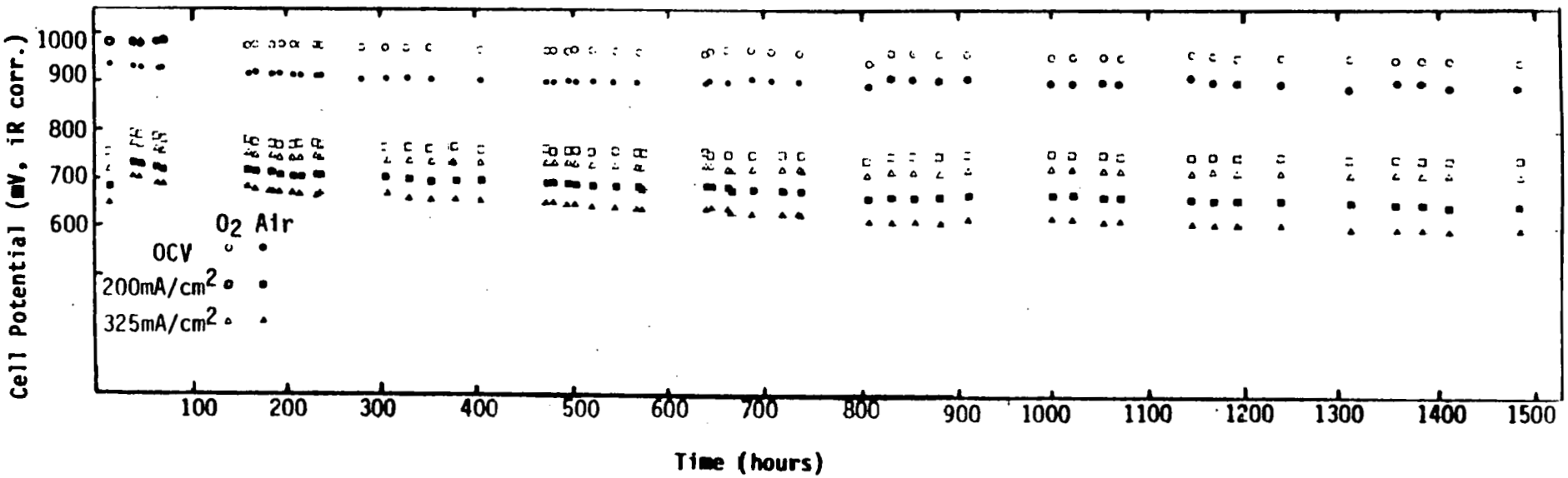

Figure 5-5. Voltage Stability of Fuel Cell Containing Pt-Cr-C Electrocatalyst at Open Circuit, 200 mA/cm² and 325 mA/cm² on Oxygen and Air at 190°C

TABLE 5-V

OXYGEN REDUCTION PERFORMANCE (iR CORRECTED) AT VARIOUS CURRENT DENSITIES IN 2" x 2" FUEL CELLS WITH ELECTROCATALYSTS Pt-Cr-Ce AND Pt-Cr-C

Electrocatalyst	Polarization (mV)				
	10 mA/cm²	20 mA/cm²	100 mA/cm²	200 mA/cm²	400 mA/cm²
Pt-Cr-Ce 21 hrs	907	878	809	777	739
1192 hrs	865	843	780	744	696
Δ	-42	-35	-29	-33	-43
Pt-Cr-C 21 hrs	913	883	815	785	752
1192 hrs	871	848	784	746	699
Δ	-42	-35	-31	-39	-53

5.4 ALLOYS WITH LANTHANUM, YTTRIUM AND URANIUM

Task I: Materials Selection

The Engle-Brewer theory was used to select both lanthanum and yttrium as candidate alloy materials. The theory is based on optimizing available "d" electrons for bonding in transition metal alloys (19). Platinum should interact most strongly, and hence, one may speculate, have the greatest stability, with lanthanum and yttrium. Uranium was selected based on a Pt_3U intermetallic prepared at Los Alamos National Laboratory.

In order to study the effect of platinum content on platinum alloy catalyst activity, four alloys with varying platinum to lanthanum ratios were selected. The platinum compositions were 85, 70, 55 and 40 atomic percent. Alloys containing uranium and yttrium carbides were also selected for preparation.

Task II: Catalyst Preparation

A series of four Pt-La/Vulcan XC-72 electrocatalysts was prepared with platinum compositions of 85, 70, 55 and 40 atomic percent using the following procedure: 10% Pt-Vulcan was dispersed in chilled water, to which was added a solution of $La(NO_3)_3 \cdot 6H_2O$, followed by the addition of sodium hydroxide to raise the pH to 11.5, thus precipitating the La. The resulting slurry was then filtered and

dried. To facilitate alloying, the sample was heated under nitrogen at 900°C for one hour.

This procedure was also used to prepare Pt-U and Pt-Y alloys, substituting $UO_2(NO_3)\cdot 6H_2O$ or $Y(NO_3)_3\cdot 6H_2O$ for the $La(NO_3)_3\cdot 6H_2O$. From these catalysts, the standard carbiding procedure was used to prepare Pt-U-C and Pt-Y-C alloys.

The Pt-U-Y alloy was prepared in a two-step process. The Pt-U alloy was prepared initially, including the 900°C heat-treatment. This material was then dispersed in distilled water and $Y(NO_3)_3\cdot 6H_2O$ added, followed by precipitation of the Y and subsequent heat-treatment for alloy formation.

Task III: Characterization and
Task IV: Electrochemical Characterization

The lattice parameters determined from the XRD analysis of the Pt-La alloys on Vulcan XC-72 are summarized in **Table 5-VI**: the lattice parameters were based on the (111) peak only. The lattice parameter for the electrocatalyst containing 85% Pt, 3.918 Å, has been observed previously for Pt/Vulcan. This fact, and the presence of a symmetrical diffraction peak profile are evidence of a homogeneous single phase. The data suggests little, if any, alloying took place.

TABLE 5-VI

EFFECT OF Pt CONTENT ON LATTICE PARAMETER OF Pt-La ELECTROCATALYST

% Pt	a_o (Å)
85	3.918
70	3.996
60	3.996
40	3.996

The lattice parameters for the other three Pt-La electrocatalysts all showed an expansion relative to that of Pt. Also, the (220) peak completely disappeared from the XRD pattern, and several new peaks occurred. The (111) peak changed from a symmetrical to an asymmetric shape with an increase in La content. The asymmetric peak is indicative of a phase separation. Evidently a non-homogeneous system was being formed with an excess of La present.

Lattice parameters for the Pt-U, Pt-Y, Pt-U-C, Pt-Y-C, Pt-U-Y and Pt-U-Y-C electrocatalysts were not measured.

Table 5-VII summarizes the results of surface areas determined by electrochemical hydrogen adsorption for the four Pt-La alloys, Pt-U, Pt-U-C, Pt-Y, Pt-Y-C, Pt-U-C and Pt-U-Y-C. Except for the Pt-U alloy, all surface areas are in the ranges observed for 900°C heat-treated material. As expected, the surface areas of the carbided electrocatalysts are smaller than those of the non-carbided precursors, reflecting the additional 900°C heat-treatment.

Also summarized in Table 5-VII are floating electrode half-cell results obtained using these materials. Although an improvement in performance, relative to that of 10% Pt/Vulcan, was observed in some cases, the improvements were of such a small magnitude that additional testing of these materials was not justified.

TABLE 5-VII

CHARACTERIZATION RESULTS

Electrocatalyst	Surface Area (m^2/g)	iR-Free Performance* at 200 mA/cm^2 (mV)	
		O_2	Air
Pt-La (85% Pt)	58	758	687
Pt-La (70% Pt)	69	739	675
Pt-La (60% Pt)	68	728	689
Pt-La (40% Pt)	51	735	678
Pt-U	117	765	695
Pt-U-C	43	729	672
Pt-Y	80	760	695
Pt-Y-C	54	752	684
Pt-U-Y	67.5	740	668
Pt-U-Y-C	35	716	623

***Test Conditions**: Floating Electrode Half-Cell, 100% H_3PO_4 at 200°C

5.5 ALLOYS WITH NICKEL AND COBALT

Task I: Material Selection

Based on bulk alloy phase diagrams, both nickel and cobalt, when alloyed with platinum, have a nearest neighbor distance smaller than that observed for platinum only (see Figure 2-1). Therefore, these materials were expected to provide high activity platinum alloys.

Task II: Preparation

The Pt-Ni, Pt-Co and Pt-Ni-Co alloys were all prepared by the standard method, i.e., precipitation of metal oxides (or hydroxides) onto a platinized support. The initial efforts were performed using Vulcan XC-72 as a support; additional efforts, directed at the preparation of high activity platinum ternary alloys on corrosion-resistant supports, included SAB, HTV, and HTBP as support materials.

Task III: Characterization

Characterization data for the Pt-Ni, Pt-Co and Pt-Ni-Co alloys on various supports is summarized in **Table 5-VIII**. Data for Pt/Vulcan has also been included for reference. All the alloys listed in the table exhibited a contraction in lattice parameter, relative to that of Pt; the decrease suggests alloy formation.

TABLE 5-VIII

CHARACTERIZATION DATA OF Pt-Ni, Pt-Co AND Pt-Ni-Co ELECTROCATALYSTS

Electrocatalyst	Lattice Parameter (Å)	Surface Area (m^2/g)
Pt	3.918	130
Pt-Ni	3.826	40
Pt-Co	3.852	41
Pt-Ni-Co	3.840	58
Pt-Ni-Co/SAB	3.843	74
Pt-Ni-Co/HTV	3.843	42
Pt-Ni-Co/HTBP	3.864	76

Several of the electrocatalysts were examined by TEM; also examined was a non-heat-treated Pt-Ni-Co/Vulcan sample. For the non-heat-treated material, the catalyst particle spatial distribution was non-uniform, with catalyst particles congregating in crevices between the support particles. The average catalyst particle size was on the order of 25 Å. For Pt-Ni-Co/Vulcan which had been heat-treated at 900°C, a bimodal average particle diameter of 30 and 60 Å was observed, with the smaller catalyst particles tending to congregate in areas of light loadings.

Examination of Pt-Ni-Co/HTV revealed a randomly selected group of catalyst particles with a mean diameter of 60 ±15 Å. The particle distribution was spatially non-uniform. Finally, examination of Pt-Ni-Co/HTBP revealed an average particle diameter of 40 ±19 Å and a very broad particle size distribution.

Task IV: Electrochemical Characterization

The electrocatalysts listed in Table 5-VIII were fabricated into standard gas diffusion electrodes and evaluated for cathode activity in the floating electrode half-cell apparatus; results are summarized in **Table 5-IX**. All electrocatalysts showed an increase in half-cell performance, relative to that of the various 10% Pt/carbon support starting materials. The highest performance was observed for the Pt-Ni-Co/Vulcan electrocatalyst. The performance of this electrocatalyst on air was the highest half-cell performance observed for an electrocatalyst evaluated during this program. Further discussion of the Pt-Ni-Co system will be deferred until Section 6.0.

TABLE 5-IX

HALF-CELL PERFORMANCE OF Pt-Ni, Pt-Co AND Pt-Ni-Co ELECTROCATALYSTS

Electrocatalyst	iR-Free Performance* at 200 mA/cm² (mV)	
	O_2	Air
Pt	745	685
Pt-Ni	761	697
Pt-Co	788	735
Pt-Ni-Co	801	740
Pt-Ni-Co/SAB	770	705
Pt-Ni-Co/HTV	758	682
Pt-Ni-Co/HTBP	772	693

***Test Conditions:** Floating Electrode Half-Cell, 100% H_3PO_4 at 200°C

5.6 ALLOYS PREPARED FROM ORGANOMETALLIC PRECURSORS

Task I: Material Selection

During the course of this program, evidence obtained from Lawrence Berkeley Laboratory suggested the presence of substantial quantities of base metal oxides in our platinum alloy electrocatalysts. The role of the metal oxides on the enhancement/degradation of

electrocatalyst stability was unknown. Therefore, a program was undertaken to prepare electrocatalysts by a method which should avoid the formation of metal oxides, namely, the deposition of base metals on an electrocatalyst support using organometallic precursors dissolved in aprotic solvents. The bulk of our efforts were directed at either the deposition of platinum itself, or the simultaneous deposition of platinum and cobalt onto non-platinized HTBP support.

Task II: Electrocatalyst Preparation

Essentially the same procedure was followed for all preparations. An organometallic compound such as platinum acetyl acetonate was dissolved in either chloroform or benzene; the desired electrocatalyst support was soaked in the solvent, followed by separation of support and solvent, drying and heat-treatment to decompose the organometallic and, where appropriate, promote alloy formation. Where necessary, multiple adsorption steps were utilized to deposit the required amount of electrocatalyst.

Task III: Characterization

Our efforts were concentrated on the preparation and characterization of Pt/HTBP and Pt-Co/HTBP by means of organometallic materials. Characterization data for these materials are summarized in **Table 5-X**. Also included in this table are the expected compositions for these three materials; good agreement was found between the expected and actual composition, demonstrating the success that can be obtained using this preparation procedure.

TEM analysis was conducted on the three electrocatalysts, with results summarized in Table 5-X; the large difference in particle diameter between the Pt and Pt-Co electrocatalysts is not understood.

TABLE 5-X

ORGANOMETALLIC ELECTROCATALYST CHARACTERIZATION RESULTS

Electrocatalyst	Expected Composition	Actual Composition	Particle Diameter (Å)
Pt/HTBP	10% Pt	8.4% Pt	60
Pt-Co/HTBP	90:10 mole ratio	93:7	33
Pt-Co/HTBP	80:20 mole ratio	86:14	35

Task IV: Electrochemical Characterization

Gas diffusion electrodes were fabricated from all three electrocatalysts and evaluated for cathode activity in the floating electrode half-cell; these materials had been subjected to both a 500 and a 900°C heat-treatment during preparation. In addition, gas diffusion electrodes were fabricated from materials heat-treated only at 500°C. Results of all testing are summarized in **Table 5-XI**.

TABLE 5-XI

HALF-CELL RESULTS, "OXIDE-FREE" ELECTROCATALYST

Electrocatalyst	Heat-Treatment Temperature (°C)	iR-Free Performance* at 200 mA/cm² (mV) O_2	Air
Pt-Co (90:10)	500, 900	768	683
Pt-Co (80:20)	500, 900	788	705
Pt	500, 900	764	670
Pt-Co (90:10)	500	740	644
Pt-Co (80:20)	500	754	669
Pt	500	742	650

***Test Conditions**: Floating Electrode Half-Cell, 100% H_3PO_4 at 200°C

A substantial increase in half-cell performance with 900°C heat-treatment was observed for all three electrocatalysts. Two synergistic effects are probably occurring to provide the increase in performance. As discussed in Section 7.0, Pt alloy formation (performed at 900°C) can result in an increase of over 50 mV in half-cell performance relative to unalloyed, non-heat-treated platinum. Likewise, it has also been shown that 900°C heat-treatment of platinum only can result in at least a 20 mV increase in performance. Since alloy formation is effected at 900°C, the increase in performance due to 900°C heat-treatment only and due to alloy formation only cannot easily be separated. For the 500°C heat-treatment temperature, performance of the Pt and 90:10 Pt-Co electrocatalysts was approximately the same; slightly higher performance was observed for the 80:20 Pt-Co. Subsequent to 900°C heat-treatment, the electrocatalysts containing Co had a larger increase in performance than the Pt-only electrocatalysts, suggesting the additional improvement in performance was due to alloy formation.

5.7 ALLOYS PREPARED WITH NON-METALLIC ADDITVES

Several attempts were made to prepare and evaluate platinum alloys containing either sulfur, boron or phosphorus. Floating electrode half-cell testing of these materials yielded a negligible performance improvement relative to that of platinum. No further discussions of these materials will be made.

5.8 CONCLUSIONS

Of all the electrocatalysts prepared and tested during this program, the Pt-Cr-Ce and Pt-Ni-Co systems yielded the highest performance in the floating electrode half-cell testing (805 O_2, 735 air for Pt-Cr-Ce and 801 O_2, 740 air for Pt-Ni-Co). Due to the higher air performance and to its simpler preparation procedure, the Pt-Ni-Co system was selected for further study and optimization. Results of this study are presented in Section 6.0.

5.9 REFERENCES FOR SECTION 5.0

1. Jalan, V. "Catalysts with Reduced Rate of Recrystallization and Methods for Making," U.S. Patent 4,137,372 (1979).

2. Jalan, V. "High Activity Platinum Catalyst and Method for Making," U.S. Patent 4,137,373 (1979).

3. Konig, H., *Naturierss.*, **38**, 154 (1951).

4. Whitcomb, M.J., V. Dalmen and K.H. Westmacott, *Acta Met.*, **31**, 743 (1983).

5. Jalan, V. "Noble Metal-Vanadium Alloy Catalysts and Method for Making," U.S. Patent 4,202,934 (1980).

6. Landsman, D. and F. Luczak, "Noble Metal-Chromium Alloy Catalysts and Electrochemical Cell," U.S. Patent 4,316,944 (1982).

7. Cormack, D., et al., *J. Catalysis*, **32**, 492 (1972).

8. Moss, R. and H. Gibbens, *J. Catalysis*, **24**, 48 (1972).

9. Moss, R., et al., *J. Catalysis*, **16**, 117 (1970).

10. Bronger, W. and W. Klemm, *Z. Anorg. Chem.*, **319**, 58 (1962).

11. Huch, R. and W. Klemm, *Z. Anorg. Chem.*, **329**, 123 (1964).

12. Maldonado, A. and K. Schubert, *Z. Metalk.*, **55**, 619 (1964).

13. Ross, P.N., National Fuel Cell Seminar, San Diego, CA, July 14-16, 1980.

14. Ross, P.N., EPRI Final Report for Contract RP 1200-5, March 1980.

15. Meschter, P.J. and W.L. Worrell, *Metallurgical Transactions*, **7a**, 299 (1976).

16. Raub, E. and G. Falkenberg, *Metall.*, **27** 669 (1973).

17. Nishimura, H. and T. Hiramatsu, *Nippon Kinzoku Gakkaishi*, **21**, 469 (1957).

18. Jalan, V. and E.J. Taylor, "Importance of Interatomic Spacing in the Catalytic Reduction of Oxygen in Phosphoric Acid," Abstract No. 729, Electrochemical Society Meeting, San Francisco, CA, May 8-13, 1983.

19. Brewer, L. in Phase Stability in Metals and Alloys, P. 39, P. Rudman, J. Stringer and R. Jaffee, eds., Mcgraw-Hill, NY (1967).

6.0 OPTIMIZATION OF Pt-Ni-Co SYSTEM

6.1 INTRODUCTION

As shown in the previous chapter, the Pt-Ni-Co/Vulcan electrocatalyst system demonstrated the highest floating electrode half-cell performance observed for a platinum ternary electrocatalyst, and also demonstrated good stability under fuel cell test conditions. Therefore, a series of experiments was conducted to optimize this electrocatalyst, in terms of improved performance and stability. Results of the optimization study are reported in this chapter. Unless otherwise stated, Vulcan XC-72 was used as the electrocatalyst support.

6.2 OPTIMIZATION VARIABLES STUDIED

6.2.1 Effect of Alloy Component Ratio

A series of electrocatalysts was prepared in which the platinum content was held constant, but the ratio of Ni to Co was varied to determine an optimum Ni to Co ratio. The mole ratios of the various electrocatalysts evaluated in this study are listed in **Table 6-I**. Also included, for completeness, are the Pt-Ni and Pt-Co binary electrocatalysts.

TABLE 6-I

EFFECT OF ALLOY COMPONENT RATIO

Mole Percent Pt:Ni:Co	iR-Free Performance* at 200 mA/cm² (mV) O_2	Air	Surface Area (m^2/g)	Lattice Parameter (Å)
70:30:0	792	733	40	3.826
70:27:3	796	734	53	3.854
70:22.5:7.5	787	722	65	3.848
70:15:15	801	740	76	3.840
70:10:20	775	713	54	3.831
70:7.5:22.5	793	727	57	3.846
70:3:27	793	731	62	3.851
70:0:30	788	735	41	3.852

***Test Conditions**: Floating Electrode Half-Cell, 100% H_3PO_4 at 200°C

All electrocatalysts were fabricated into electrodes and evaluated for cathode activity in the floating electrode half-cell apparatus.

Results of these experiments, with data for both O_2 and air, are summarized in Table 6-I, and plotted in **Figure 6-1**. Maximum voltages (at 200 mA/cm²) were observed for the electrocatalyst having a 70:15:15 ratio of Pt-Ni-Co. This composition was that of the electrocatalyst designated G82-5-19. Figure 6-1 shows the performance of this series of electrocatalysts did not vary greatly over a wide range of Ni:Co mole ratios, but a definite peak in performance was observed at the 70:15:15 ratio.

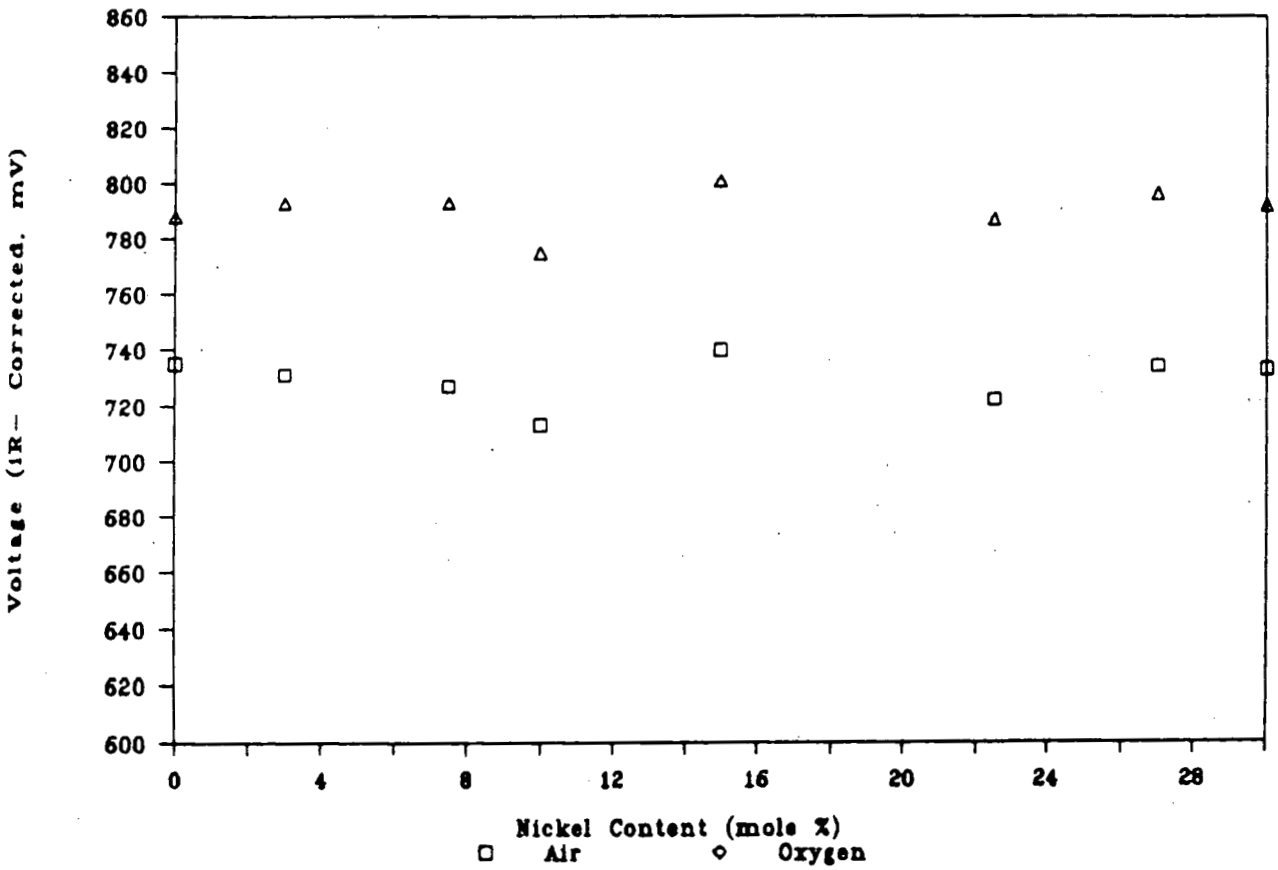

Figure 6-1. Effect of Increasing Ni Content on Floating Electrode Half-Cell Performance

Electrochemical surface areas were also measured and are listed in Table 6-I. Most of the surface areas fall within the range of previously observed values for electrocatalyst which had been subjected to 900°C heat-treatment.

Lattice parameters were calculated from XRD patterns for the various electrocatalysts and are summarized in the last column of Table 6-I. Symmetric peaks were observed in all cases. Only a small change in lattice parameter was observed.

These experiments suggested that the optimum component ratio was 70:15:15.

6.2.2. Effect of Pt:(Alloy Component) Ratio

The experiments described in Section 6.2.1 suggested an optimum alloy component ratio of 70:15:15, or an optimum Ni:Co ratio of 1:1. Using this 1:1 ratio, another series of electrocatalysts was prepared. In this case, the Ni:Co ratio was held constant at 1:1 while the ratio of Pt:(Ni + Co) was varied. The compositions of the electrocatalysts prepared and evaluated are listed in **Table 6-II**. Also included in this Table are data for the 70:15:15 ratio; these data were obtained from the previous set of experiments.

Half-cell testing of this group of electrocatalysts, with results listed in Table 6-II and plotted in **Figure 6-2**, again suggested the 70:15:15 ratio yielded the best performance.

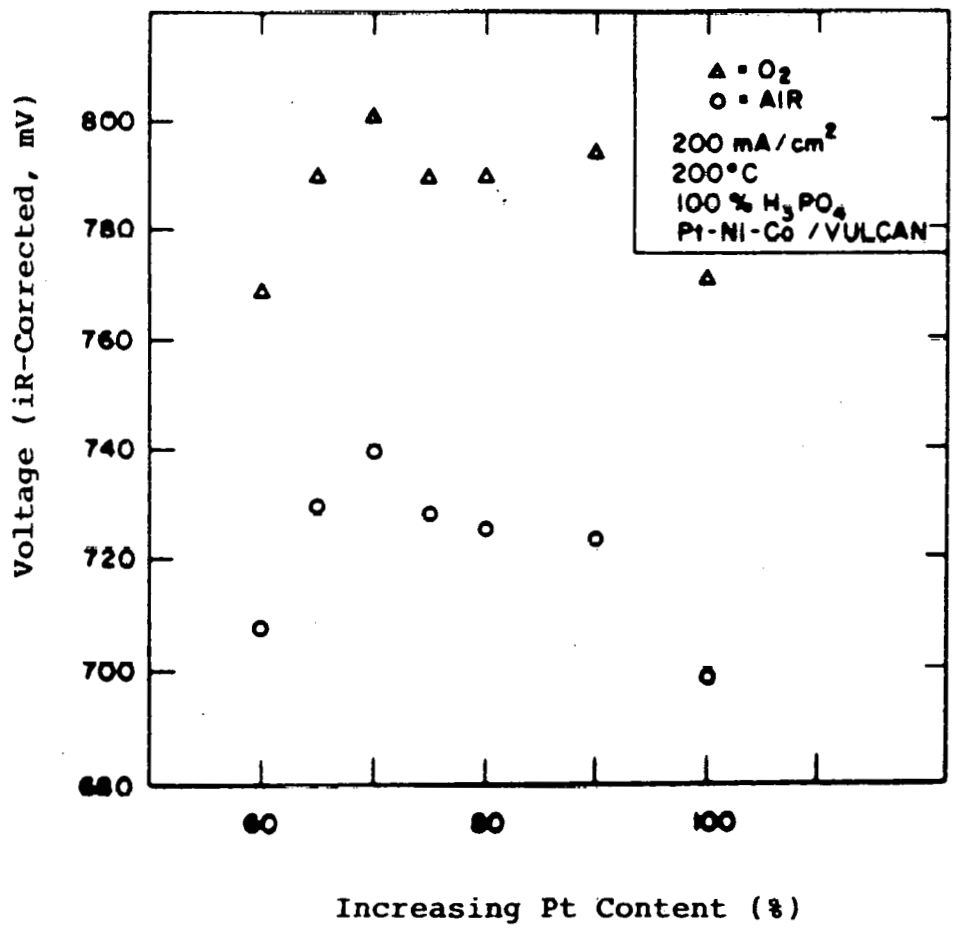

Figure 6-2. Effect of Increasing Pt Content on Floating Electrode Half-Cell Performance

TABLE 6-II

VARIATION OF Pt:(Ni + Co) RATIO

MOLE PERCENT Pt:Ni:Co	iR-Free Performance* at 200 mA/cm² (mV) O_2	Air	Gain	Surface Area (m^2/g)	Lattice Parameter (Å)
60:20:20	774	708	66	52	3.820
65:17.5:17.5	790	730	60	68	3.807
70:15:15	801	740	61	76	3.840
75:12.5:12.5	790	729	61	78	3.826
80:10:10	791	726	65	54	3.886
90:5:5	794	724	70	61	3.902
100:0:0	745	685	60	130	3.918

***Test Conditions**: Floating Electrode Half-Cell, 100% H_3PO_4 at 200°C

Surface area data are also summarized in Table 6-II, with observed values again consistent with those seen previously for 900°C heat-treated electrocatalyst.

Lattice parameters were calculated from XRD data and are summarized in the last column of Table 6-II. Symmetric peaks were observed in all cases. The general trend appears to be an increase in lattice parameter with an increase in platinum content. This is expected as there is less material to alloy with the platinum. In all cases, the platinum loading was held constant at 0.5 mg/cm² while the amount of Ni and Co deposited onto the platinized support was decreased. As with the results obtained in Section 6.2.1, an alloy component ratio of 70:15:15 yielded the best performance.

6.2.3. Order of Component Deposition

The standard preparation procedure for the Pt-Ni-Co/Vulcan electrocatalyst involves the simultaneous deposition of Ni and Co oxide (hydroxide) onto a platinized support. Two variations of this procedure were evaluated, to determine their effect on electrocatalyst performance. For the G82-5-44 electrocatalyst, platinized Vulcan was impregnated with Co, heat-treated for 1 hour at 900°C under

N_2, impregnated with Ni and heat-treated again. In the case of the G82-5-45 electrocatalyst, the platinized Vulcan was impregnated with Co, then impregnated with Ni and finally subjected to 900°C heat-treatment.

Gas diffusion electrodes were fabricated from each electrocatalyst and standard evaluation procedures utilized. Results are summarized in **Table 6-III**; results obtained using electrocatalyst prepared by the standard procedure are included for comparison purposes. These results suggest that the manner in which the alloy components are deposited on the platinized substrate has an effect on the overall performance of the electrocatalyst. The decrease in performance observed for the G82-5-44 electrocatalyst was due to the two, 900°C heat-treatments, resulting in decreased surface area. The drop in performance for the G82-5-45 electrocatalyst is not completely understood, but may be related to the manner in which the Ni and Co were distributed on the surface of the Vulcan prior to heat-treatment. The Ni and Co particles are too small to be observed via TEM, so this distribution could not be visually confirmed.

TABLE 6-III

VARIATION IN DEPOSITION ORDER

Electrocatalyst/ Prep. Method	iR-Free Performance* at 200 mA/cm² (mV)		Surface Area (m^2/g)	Lattice Parameter (Å)
	O_2	Air		
-19/Standard	801	740	76	3.840
-44/Co, HT, Ni, HT	781	711	59	3.851
-45/Co, Ni, HT	773	703	68	3.845

***Test Conditions**: Floating Electrode Half-Cell, 100% H_3PO_4 at 200°C

6.2.4 Effect of Heat-Treatment Temperature

The standard heat-treatment temperature used in alloy formation is 900°C. A study was performed to determine what effect, if any, variations in heat-treatment temperature would have on electrocatalyst performance.

A large batch of Pt-Ni-Co/Vulcan was prepared, halting the procedure just prior to the heat-treatment step. The large batch was

divided into smaller batches and each batch subjected to a one-hour heat-treatment under nitrogen at temperatures ranging from 500 to 1100°C, in 200°C increments; a portion of the electrocatalyst was set aside and utilized without heat-treatment. Similar heat-treatments were performed on batches of 10% Pt/Vulcan, to obtain baseline measurements.

Gas diffusion electrodes were fabricated from all of the above materials for both half-cell and surface area measurements; samples of the powders themselves were sent out for XRD analyses. Results of these tests are summarized in **Table 6-IV**. Several trends are immediately obvious from the data. First, O_2 performance peaks at a 900°C heat-treatment temperature. The air data for the Pt-Ni-Co alloy heat-treated at 500 and 700°C suggest these temperatures afford better performance than 900°C heat-treatment. However, inspection of the O_2 gain at 500°C and 900°C reveals that, at 500°C, the gain is much lower than would be expected*, resulting in a higher value for air performance. The gain at 900°C is higher than would normally be expected, resulting in a depressed air performance value.

The other obvious trend in the data is the decrease in surface area with increasing heat-treatment temperature. This result is expected due to increasing thermal sintering of the electrocatalyst particles with increasing heat-treatment temperature. Surface area of the Pt electrocatalyst decreased from 140 to 23 m^2/g, while that of the Pt-Ni-Co alloy initially increased from 95 to 113 m^2/g, then decreased to 17 m^2/g with increasing temperature. The decrease in Pt surface area yielded a Pt particle size increase from 20 to 122 Å, while the Pt-Ni-Co particle size increased from 29 to 165 Å, over the same temperature range.

X-ray diffraction data for the two sets of electrocatalysts are different. Heat-treatment of the Pt caused an initial increase in lattice parameter, which then decreased over the range 320 to 1100°C. By way of contrast, the lattice parameter for the Pt-Ni-Co electrocatalyst decreased from 3.918 Å (no heat-treatment) to 3.844 Å (900°C heat-treatment), then increased slightly to 3.856 Å.

The overall conclusion from this data is that 900°C heat-treatment results in optimum performance for both Pt and Pt-Ni-Co electrocatalysts.

---

* E = Tafel Slope x log[O_2 partial pressure ratio]
= 90 x log 0.21 = 61 mV

TABLE 6-IV

EFFECT OF HEAT-TREATMENT TEMPERATURE

	Pt/Vulcan				Pt-Ni-Co/Vulcan			
Temperature (°C)	iR-Free Performance* at 200 mA/cm² (mV) O_2	Air	Surface Area (m^2/g)	Lattice Parameter (Å)	iR-Free Performance* at 200 mA/cm² (mV) O_2	Air	Surface Area (m^2/g)	Lattice Parameter (Å)
NONE	746	685	140	3.918	742	684	95	3.918
320	739	678	102	3.959	---	---	--	---
450-500	744	---	111	3.955	781	730	113	3.901
600	747	680	84	3.954	---	---	--	---
700-750	759	679	87	3.951	792	730	98	3.856
900	771	699	61	3.943	795	722	74	3.844
1050-1100	760	679	23	3.943	775	713	17	3.856

*Test Conditions: Floating Electrode Half-Cell, 100% H_3PO_4 at 200°C

6.2.5 Effect of Heat-Treatment Atmosphere

Another variable evaluated during the optimization program was the atmosphere under which heat-treatment was conducted. The majority of the electrocatalysts listed previously in Chapter 3 were heat-treated for one hour in a pre-purified N_2 atmosphere. Other atmospheres evaluated during this study included 2% H_2/N_2, 2% CO/N_2 and ultrapure He.

A batch of the Pt-Ni-Co alloy electrocatalyst was prepared, divided into four smaller batches, and each small batch heat-treated under a different atmosphere. Standard evaluation tests were performed, and results summarized in **Table 6-V**.

TABLE 6-V

EFFECT OF HEAT-TREATMENT ATMOSPHERE ON ELECTROCATALYST PROPERTIES

Heat-Treatment Atmosphere	iR-Free Performance* at 200 mA/cm² (mV)		Surface Area (m^2/g)	Lattice Parameter (Å)
	O_2	Air		
Pre-purified N_2 (standard)	801	740	76	3.844
2% H_2/N_2	795	735	53	3.856
2% CO/N_2	783	725	55	3.851
Ultra-pure He	795	729	61	3.850

***Test Conditions**: Floating Electrode Half-Cell, 100% H_3PO_4 at 200°C

Use of the ultra-pure He atmosphere did not yield improved performance as compared to the standard N_2 atmosphere; use of 2% CO/N_2 appears to have had an adverse effect on performance. The air data suggest use of the ultra-pure He also had an adverse effect on half-cell performance. However, the oxygen gain observed for this electrocatalyst, which is higher than that observed for the other three, suggests part of the poor air performance is due to electrode structure problems.

6.2.6 Effect of Electrocatalyst Support

6.2.6.1 Background

In recent years two major advances in PAFC technology have been pressurized operation to obtain high system efficiency and the development of platinum alloys as high activity

cathode electrocatalysts. Both advances provide higher cathode potential and place demanding constraints on some components of the PAFC, including the electrocatalyst support. Long-term testing by various DOE contractors demonstrated the suitability of more corrosion resistant graphitized carbon blacks as electrocatalyst supports. Therefore, an emphasis was placed on the preparation of high activity platinum ternary alloys (e.g., Pt-Ni-Co) on corrosion resistant supports, followed by the fabrication of these electrocatalysts into efficient gas diffusion electrode structures. The corrosion resistant supports investigated were Shawinigan Acetylene Black (SAB), 2700°C heat-treated Vulcan XC-72 (HTV) and 2700°C heat-treated Black Pearls 2000 (HTBP); as received Vulcan XC-72 was used as a baseline.

6.2.6.2 Characterization

Platinum ternary alloys were fabricated using the above listed electrocatalyst supports. All alloys consisted of a 70:15:15 mole ratio of Pt-Ni-Co, heat-treated for 1 hour at 900°C under a nitrogen atmosphere. Electrodes were fabricated from each material and standard characterization tests performed; results of these tests are summarized in **Table 6-VI**. For comparison, results obtained using the platinized supports themselves are also listed in Table 6-VI.

TABLE 6-VI

CHARACTERIZATION OF ELECTROCATALYSTS ON CORROSION-RESISTANT SUPPORTS

Electrocatalyst	iR-Free Performance* at 200 mA/cm² (mV) O_2	Air	Gain	Surface Area (m^2/g)	Lattice Parameter (Å)
Pt/HTV	725	638	87	70	3.944
Pt-Ni-Co/HTV	758	682	76	42	3.846
Pt/HTBP	746	663	83	93	-----
Pt-Ni-Co/HTBP	775	695	80	76	3.864
Pt/SAB	745	678	67	69	3.958
Pt-Ni-Co/SAB	770	705	65	74	3.843
Pt/Vulcan	745	685	60	130	3.918
Pt-Ni-Co/Vulcan	801	740	61	74	3.844

***Test Conditions**: Floating Electrode Half-Cell, 100% H_3PO_4 at 200°C

All the electrocatalysts showed at least a 25 mV increase in performance going from Pt to the Pt-Ni-Co alloy. Except for Pt/HTV, the half-cell performance of all the platinized supports was approximately the same; it is felt lower performance was observed with Pt/HTV due to difficulties in wetting the electrocatalyst surface. The increase in performance due to alloy formation, when using HTV as a support, however, was higher than that observed for either HTBP or SAB. Except for the use of HTBP as a support, all electrocatalysts showed a decrease in lattice parameter, determined from XRD data, going from Pt to Pt-Ni-Co; this decrease suggested alloy formation. XRD data was not obtained on Pt/HTBP. Due to the larger increases in performance going from Pt to Pt-Ni-Co when using HTV and HTBP as a support, as opposed to SAB, further efforts utilizing corrosion resistant supports were limited to these two materials.

6.2.6.3 Electrode Optimization

Studies were undertaken using Pt-Ni-Co alloys supported on HTV and HTBP to determine optimum PTFE contents for gas diffusion electrode structures. In addition, sintering temperature was also examined for alloys supported on HTBP.

Gas diffusion electrodes were prepared from the Pt-Ni-Co/HTV electrocatalyst containing 20, 30, 40, 50 and 60% PTFE. These electrodes were evaluated using the floating electrode half-cell apparatus. The Tafel slopes between 10 and 100 mA/cm^2, the performances on oxygen at 200 mA/cm^2, and the oxygen gains at 200 mA/cm^2 as a function of PTFE content for these electrodes are tabulated in **Table 6-VII**. The electrode with 30% PTFE exhibited the best oxygen reduction performance characteristics—lowest Tafel slope, lowest oxygen gain, and highest performance at 200 mA/cm^2. The data indicate that 50 and 60% PTFE render the electrode too hydrophobic while 20% PTFE renders the electrode too wettable.

Stability testing of four full cells containing the Pt-Ni-Co/HTV electrocatalyst with 30, 35, and 40% PTFE content was conducted. Testing was conducted at the standard atmospheric conditions of 190°C, 50% utilization on air, and H_2 as anode gas presaturated at 72°C to maintain 100% H_3PO_4. The iR-corrected performance of these full cells as a function of time is given in **Figures 6-3, 6-4** and **6-5**. The full cells containing 30 and 35% PTFE were taken off test after 1000 and 1500 hours, respectively, due to the better performance exhibited by the full cell containing 40% PTFE. The fourth full cell also contained the Pt-Ni-Co/HTV electrocatalyst with 30% PTFE. This cell

was taken off test after 364 hours due to a rapid decay in performance. A very high O_2 gain (98 mV) observed at the 350 hour mark indicated the cathode of the cell may have flooded. Therefore, it was decided to fabricate gas diffusion electrodes supported on HTV using 40% PTFE.

TABLE 6-VII

SUMMARY OF THE EFFECT OF PTFE CONTENT ON THE iR-CORRECTED POLARIZATION BEHAVIOR OF Pt-Ni-Co/HTV

PTFE Content (wt%)	Tafel Slope (mV/decade)	O_2 Performance* at 200 mA/cm² (mV)	O_2 Gain at 200 mA/cm² (mV)
20	110	750	104
30	90	769	68
40	102	758	76
50	130	713	83
60	140	660	119

***Test Conditions:** Floating Electrode Half-Cell, 100% H_3PO_4 at 200°C

Atmospheric full cell stability testing using the HTBP support (to be described in a later section) also indicated rapid flooding of the cathode structure. Therefore, a study was conducted to determine the optimum PTFE content/sintering temperature combination for use with Pt-Ni-Co/HTBP. Four large gas diffusion electrodes were fabricated containing either 40, 45, 50 or 55% PTFE. Each large electrode was cut into three smaller pieces, and each piece sintered at either 345, 355 or 365°C for 15 minutes. This matrix of 12 PTFE content/sintering temperature combinations was evaluated under full cell pressurized conditions, with each cell being run for a total of ~250 hours.

Results of this testing are summarized in **Figure 6-6**. Plotted in this figure is the peak performance on air and performance on air after ~250 hours as a function of PTFE content. For two builds (45% PTFE/365°C and 50% PTFE/355°C), peak and final performance were identical. Overall, the highest peak performance was observed for a 345°C sinter temperature; results for the 55% PTFE/365°C combination were below 720 mV and are not plotted. Two combinations, 50%/345°C and 55%/345°C were chosen as potential candidates for electrode fabrication conditions, but were subjected to additional full cell testing prior to making a decision.

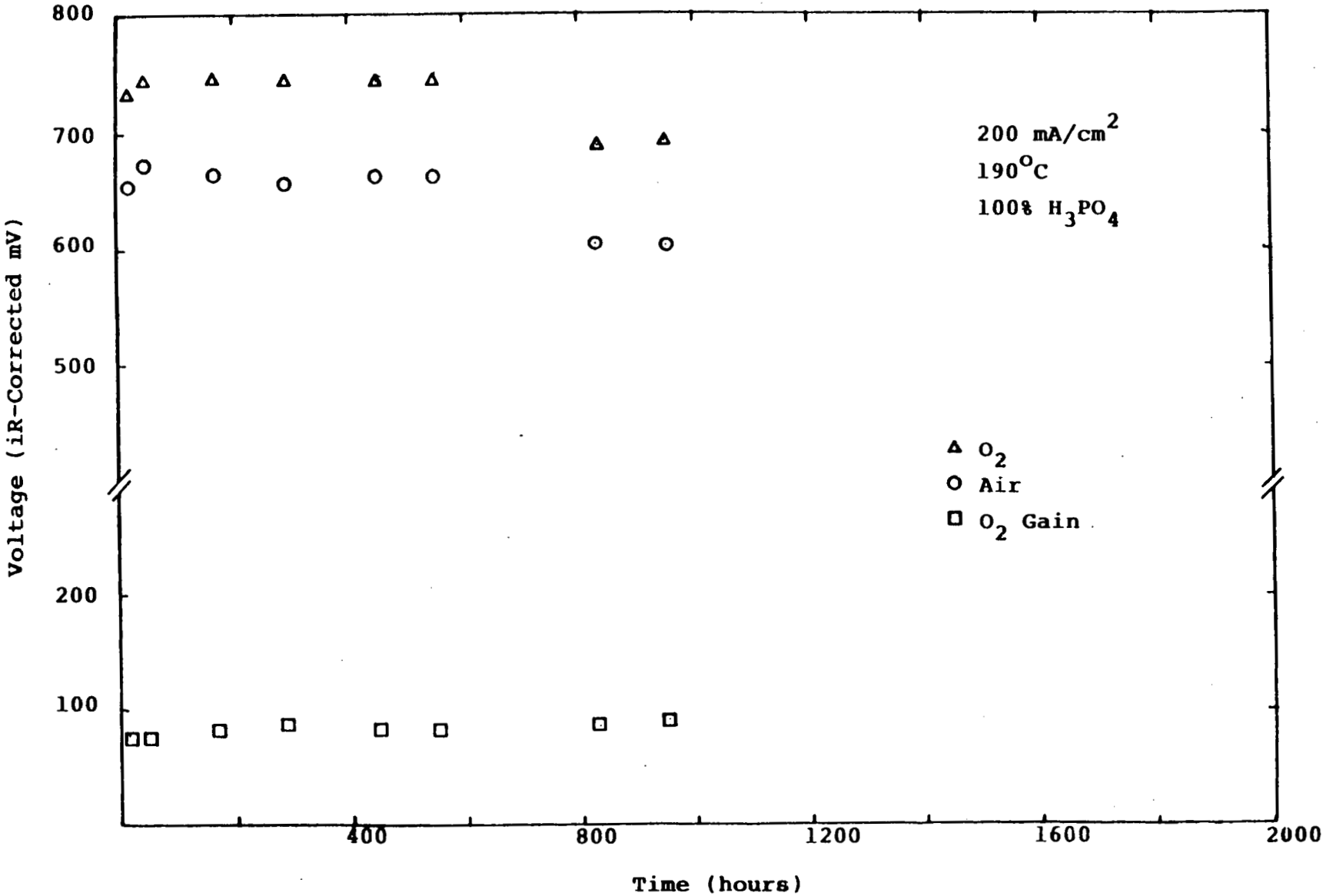

Figure 6-3. Life Performance of a Fuel Cell Containing the Pt-Ni-Co/HTV Electrocatalyst with 30% PTFE (Build 49)

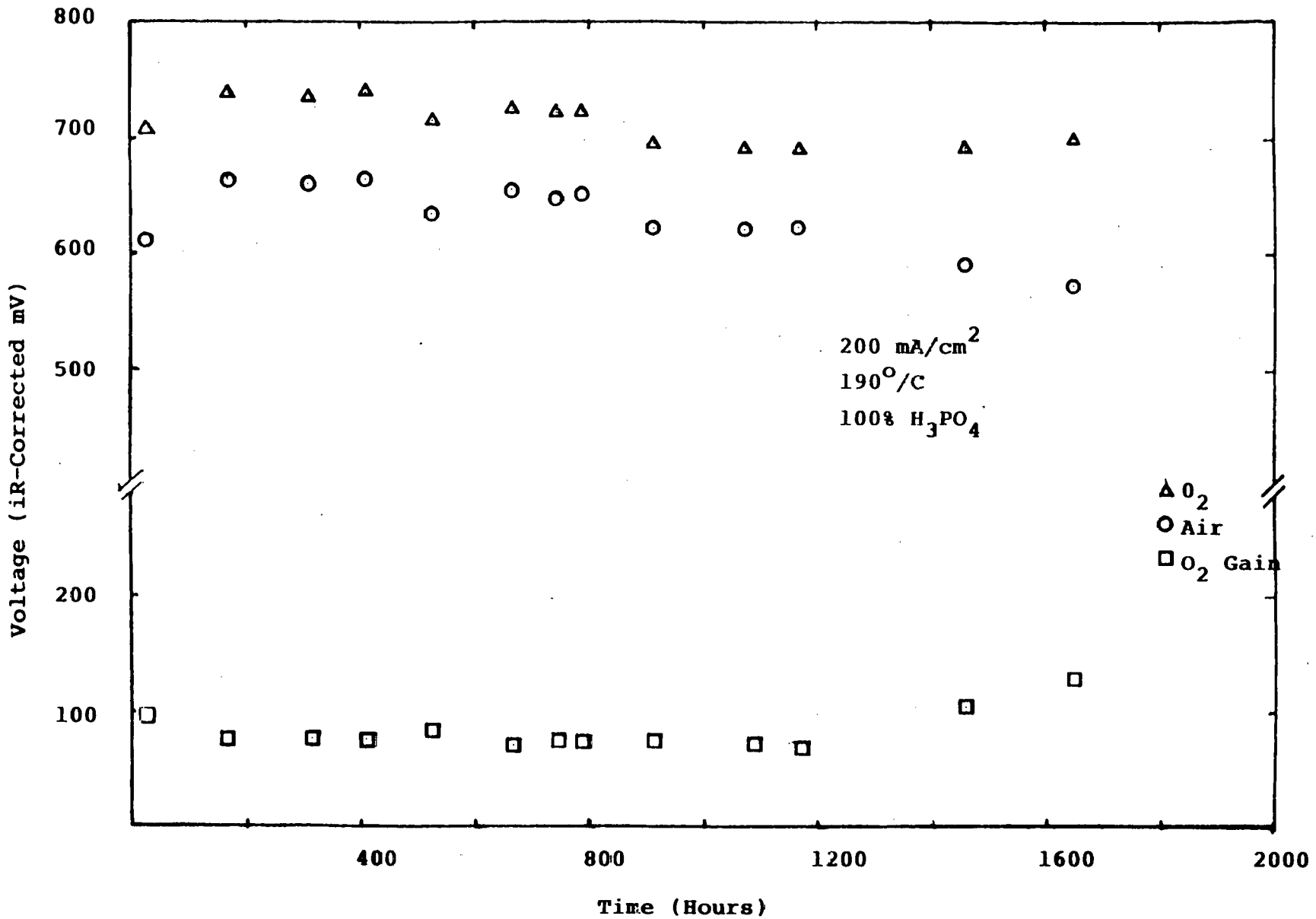

Figure 6-4. Life Performance of a Fuel Cell Containing the Pt-Ni-Co/HTV Electrocatalyst with 35% PTFE (Build 47)

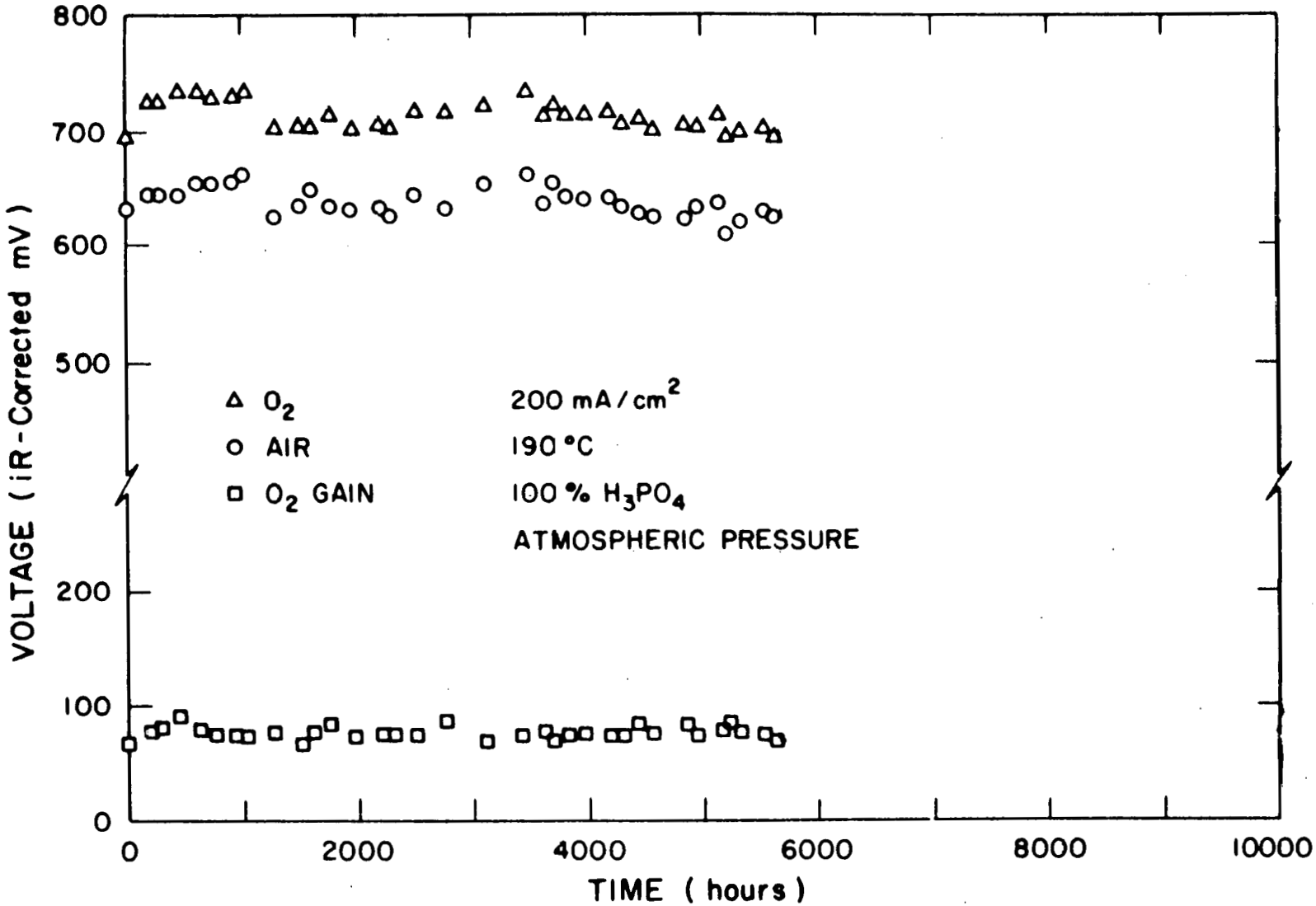

Figure 6-5. Life Performance of a Fuel Cell Containing the Pt-Ni-Co/HTV Electrocatalyst with 40% PTFE (Build 40)

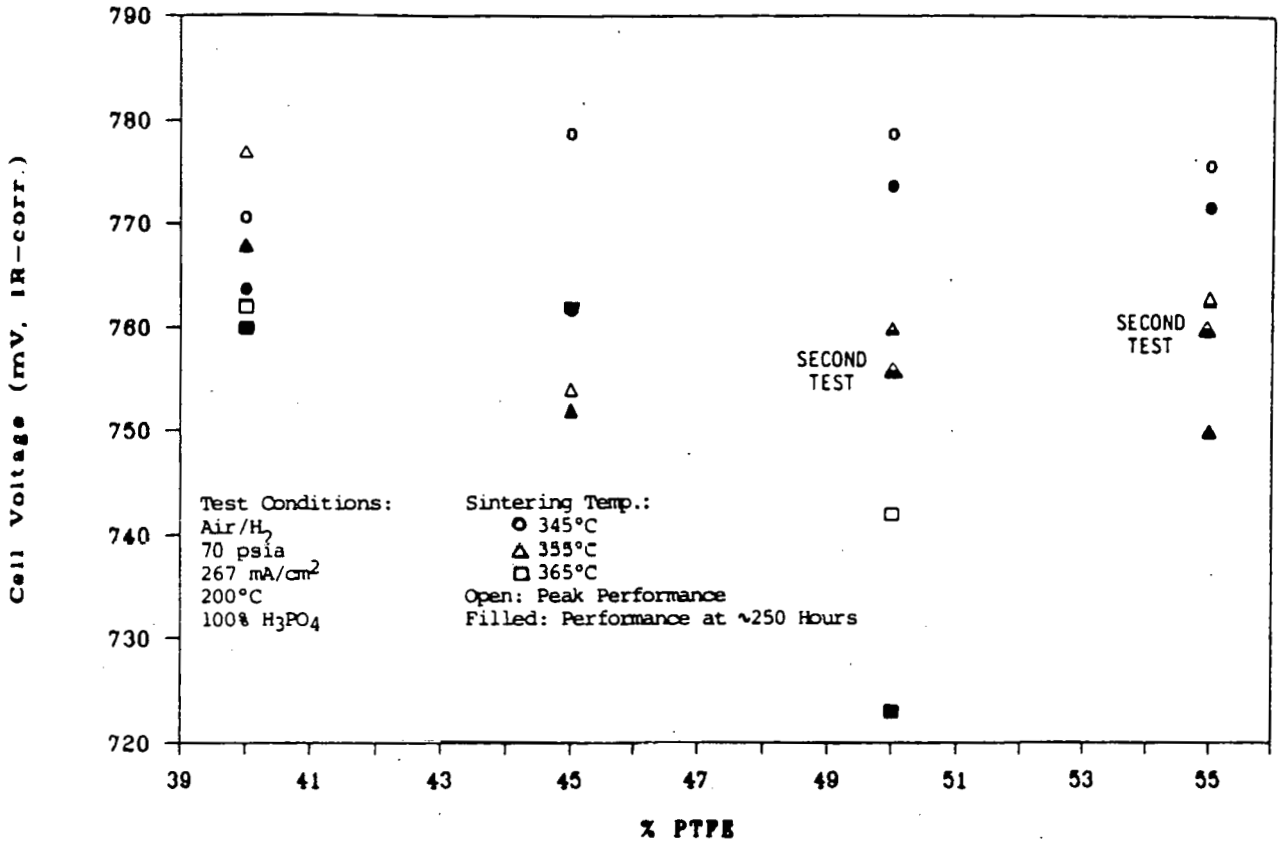

Figure 6-6. Effect of PTFE Content/Sintering Temperature on Performance

Upon retest, results were different from those obtained during the initial test. This time, peak and final performance of these two combinations were identical, with that of the 55%/345°C combination exceeding that of the 50%/345°C combination by 5 mV; these points are also plotted in Figure 6-6. However, peak performance for both builds was below that observed during the previous testing. Due to the higher performance observed for the second build containing 55% PTFE/345°C sinter, and the smaller peak to final voltage drop for the first 55%/345°C build, it was decided to select these electrode preparation conditions for use with the HTBP support.

6.3 FULL CELL STABILITY TESTING

6.3.1 Atmospheric Testing

Long-term full cell stability tests under atmospheric conditions were conducted with both the Pt-Ni-Co/Vulcan and Pt-Ni-Co/HTV electrocatalysts; results of this testing are shown in **Figures 6-7** and **6-8** for the Vulcan and HTV supports, respectively.

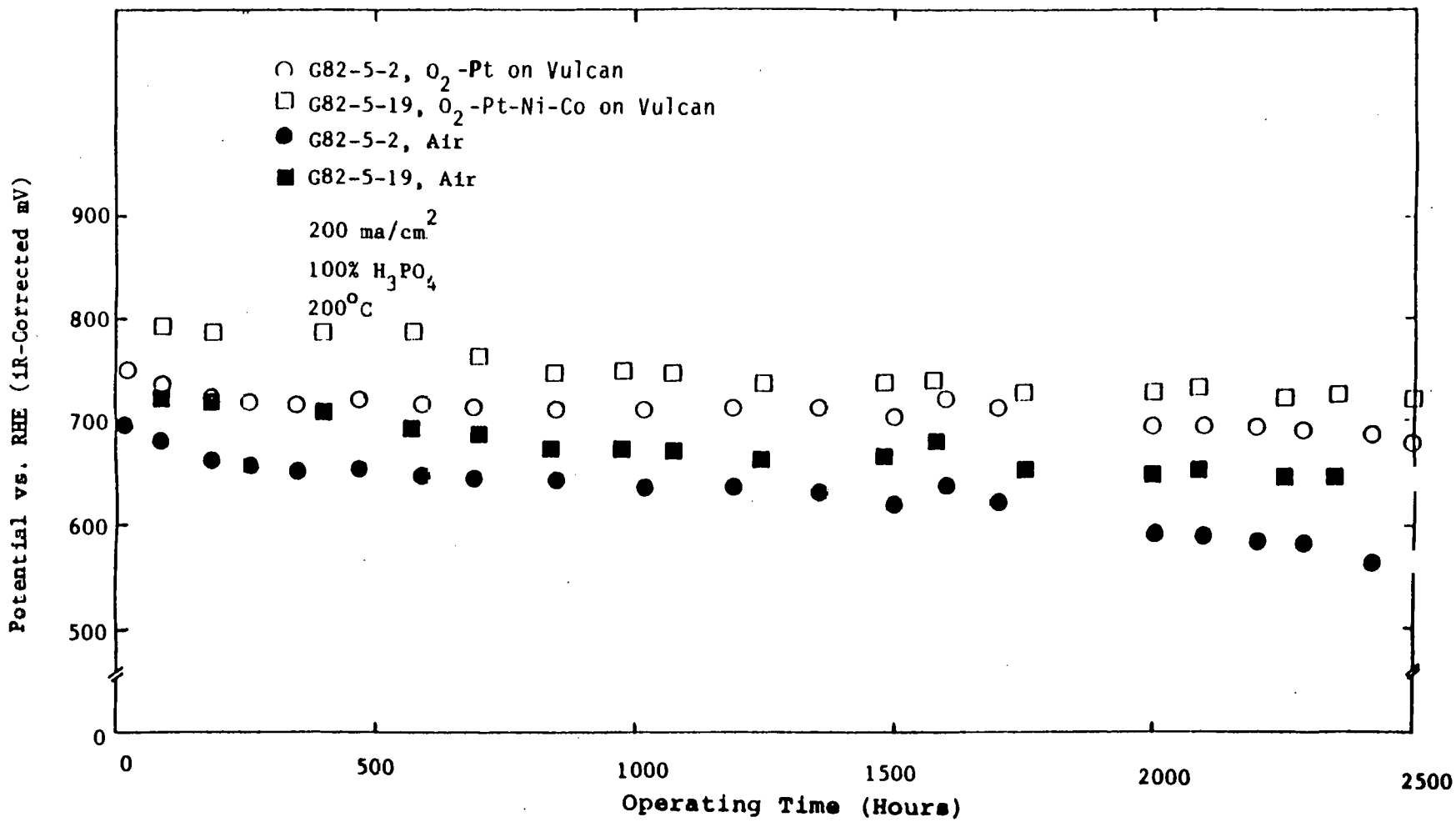

Figure 6-7. Life Performance of Fuel Cells Containing Pt-Ni-Co/Vulcan and Pt/Vulcan Cathode Electrocatalysts

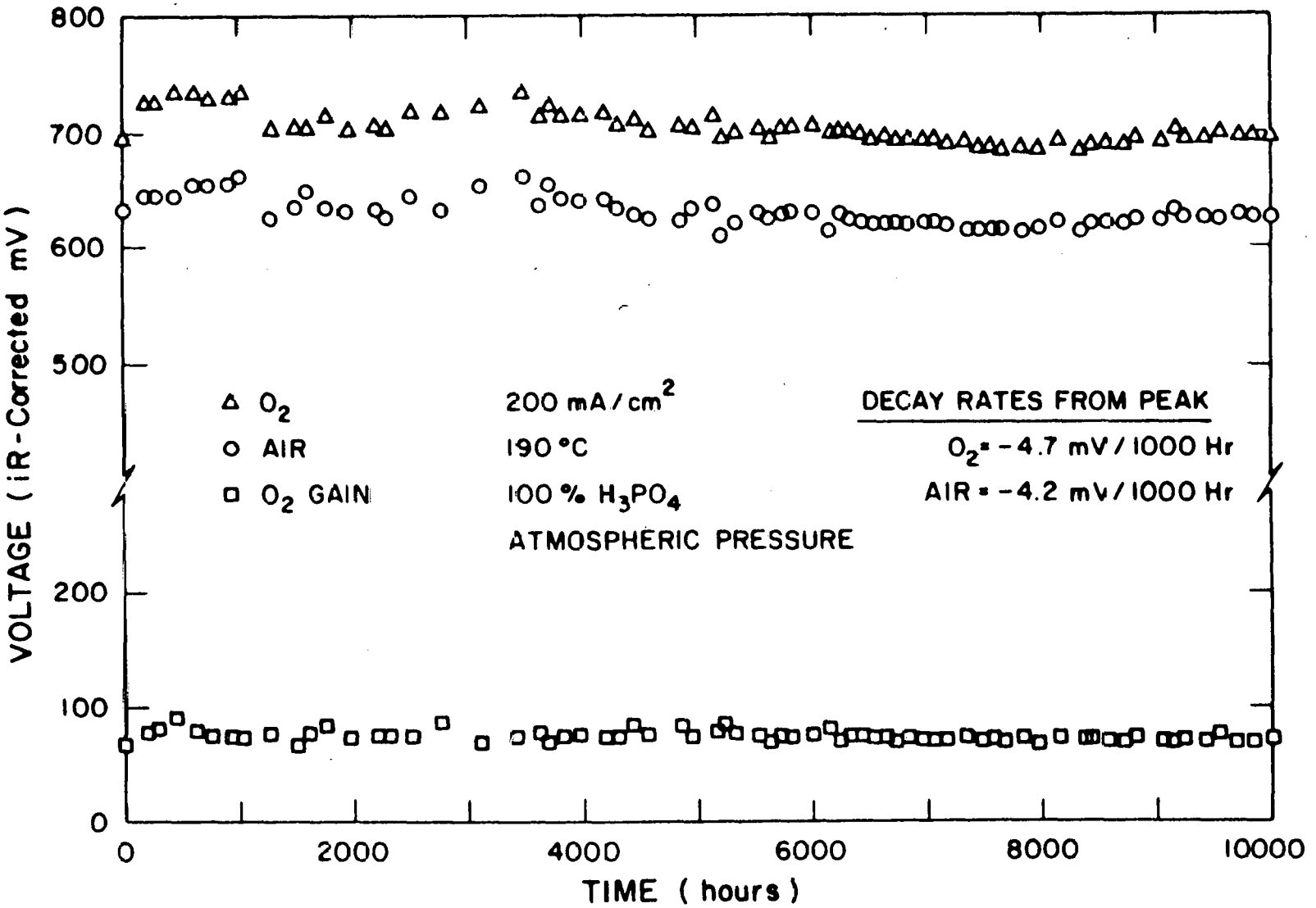

Figure 6-8. Life Performance of a Fuel Cell Containing the Pt-Ni-Co/HTV Electrocatalyst at Atmosphere Pressure (Build 40)

In Figure 6-7, results obtained with the Pt-Ni-Co/Vulcan electrocatalyst are compared with results obtained from a fuel cell which had a 10% Pt/Vulcan cathode. Over the time frame shown in Figure 6-7, the decay rates for Pt and Pt-Ni-Co are -28 and -33 mV/1000 hr, respectively. Between 500 and 900 hours of operation, the Pt-Ni-Co electrocatalyst exhibited a large performance drop. Consequently, the decay rate of the Pt-Ni-Co electrocatalyst was higher than that of the platinum standard over the 2500 hour test period; however, the decay of the Pt-Ni-Co between 2000 and 2500 hours was only 7 mV compared to 18 mV for platinum. Over the entire 2500-hour test period, performance of the Pt-Ni-Co electrocatalyst was higher than that of the platinum standard.

Figure 6-8 shows the life performance at 200 mA/cm^2 on both oxygen and air as a function of operating time for Build 40, which contained a cathode fabricated from Pt-Ni-Co/HTV. Peak performance (736 mV O_2, 640 mV air) was achieved at about the 1,000 hour mark. The observed decay rates from the peak were -4.7 mV/1,000 hours on oxygen and -4.2 mV/1,000 hours on air. Performance appears to have stabilized after the 6,000 hour mark; from the 6,000 to 10,000 hour mark, the observed decay rates were -1.3 mV/1,000 hours on oxygen and -0.5 mV/1,000 hours on air, both extremely stable performance. The observed oxygen gain remained very stable over the lifetime of the test, on the order of 70 mV.

The data presented in Figure 6-8 demonstrate that the Pt-Ni-Co/HTV electrocatalyst can provide excellent stability over at least 10,000 hours of operation at atmospheric pressure and also suggest that after 6,000 hours of operation, performance becomes even more stable.

6.3.2 Pressurized Testing

The Pt-Ni-Co/HTV and Pt-Ni-Co/HTBP electrocatalysts were also subjected to full stability testing using pressurized (267 mA/cm^2, 70 psia) test conditions. Several 1,000 hour full cell stability tests were also performed with Pt-Ni-Co/HTV but at 200 mA/cm^2 and 70 psig; results of those tests will not be discussed in detail as the operating conditions are not those envisioned for use in full scale PAFC power plants such as those being developed by Westinghouse under DOE Program DE-AC21-82MC24223.

A total of twelve full cell tests were run at 267 mA/cm², six using Pt-Ni-Co/HTV and six with Pt-Ni-Co/HTBP. Of the tests run with the HTV support, three were terminated after less than 100 hours at pressure due to operational problems. One test, Build 117, was only run for 180 hours at pressure. Air performance for this build was low, with a peak value of 720 mV. Builds 110 and 116 were run for 565 and 1,000 hours, respectively. Build 110 was shut down during a facility failure; this emergency shutdown resulted in a hole in the matrix. A life plot for Build 110 is shown in **Figure 6-9**. Performance of Build 110 was relatively stable, with an air decay rate of -8 mV/1000 hours. The observed decay rate for Build 116 was approximately twice that of Build 110, or -18 mV/1000 hours.

A life plot of a typical build with the Pt-Ni-Co/HTBP cathode electrocatalyst is shown in **Figure 6-10**. The decay rates for this build and other 1000-hour life tests (not shown) were the same order of magnitude as observed for the pressurized full cell build using the HTV support, i.e., -21 mV/1000 hours for Build 153, -18 mV/1000 hours for Build 156 and -9 mV/1000 hours for Build 157. Except for Build 153, the initial performance of the builds using the HTBP support was ~15 to 20 mV lower than that observed for the two builds using the HTV support.

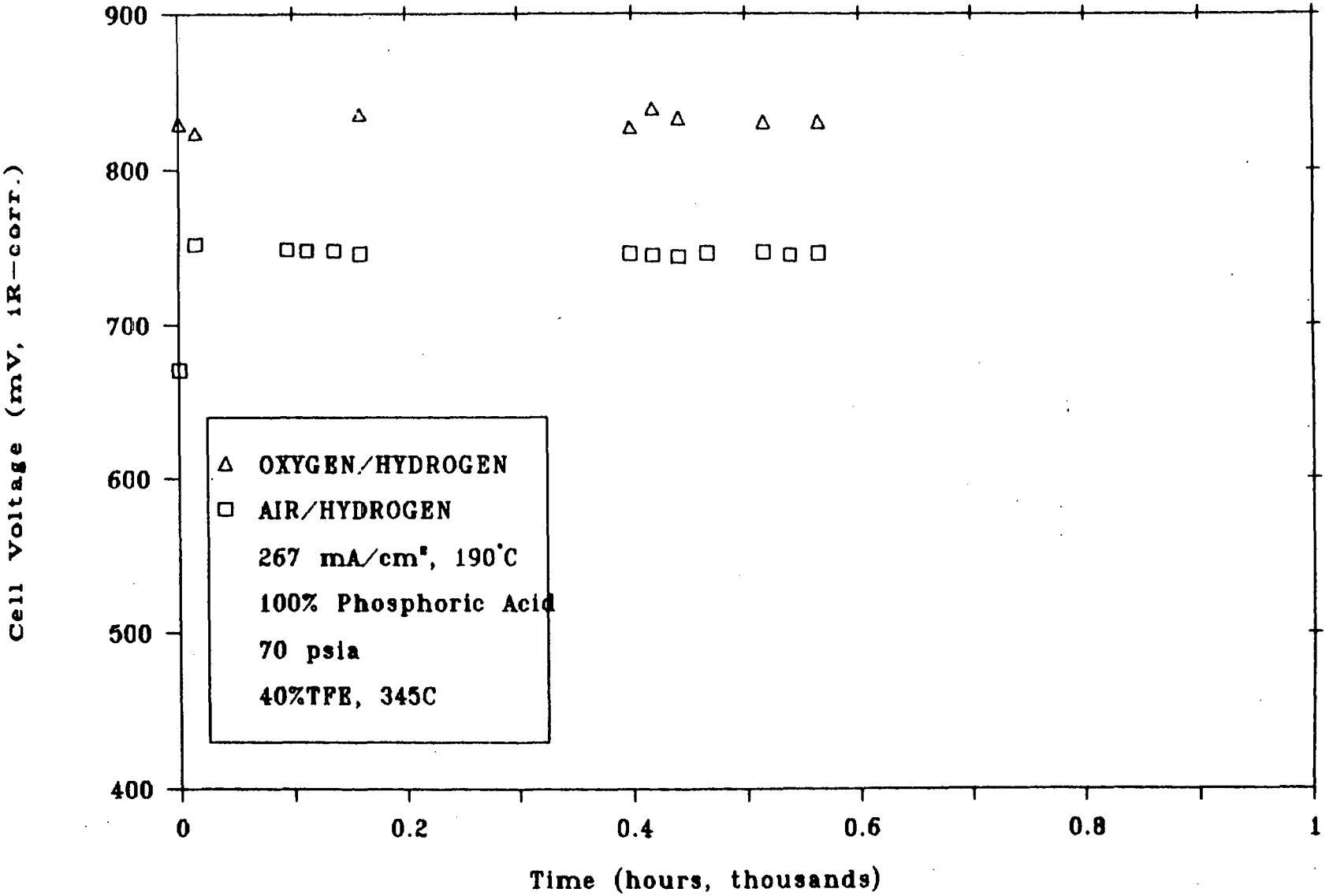

Figure 6-9. **Life Performance of a Fuel Cell Containing the Pt-Ni-Co/HTV Electrocatalyst During Pressurized Operation (Build 110)**

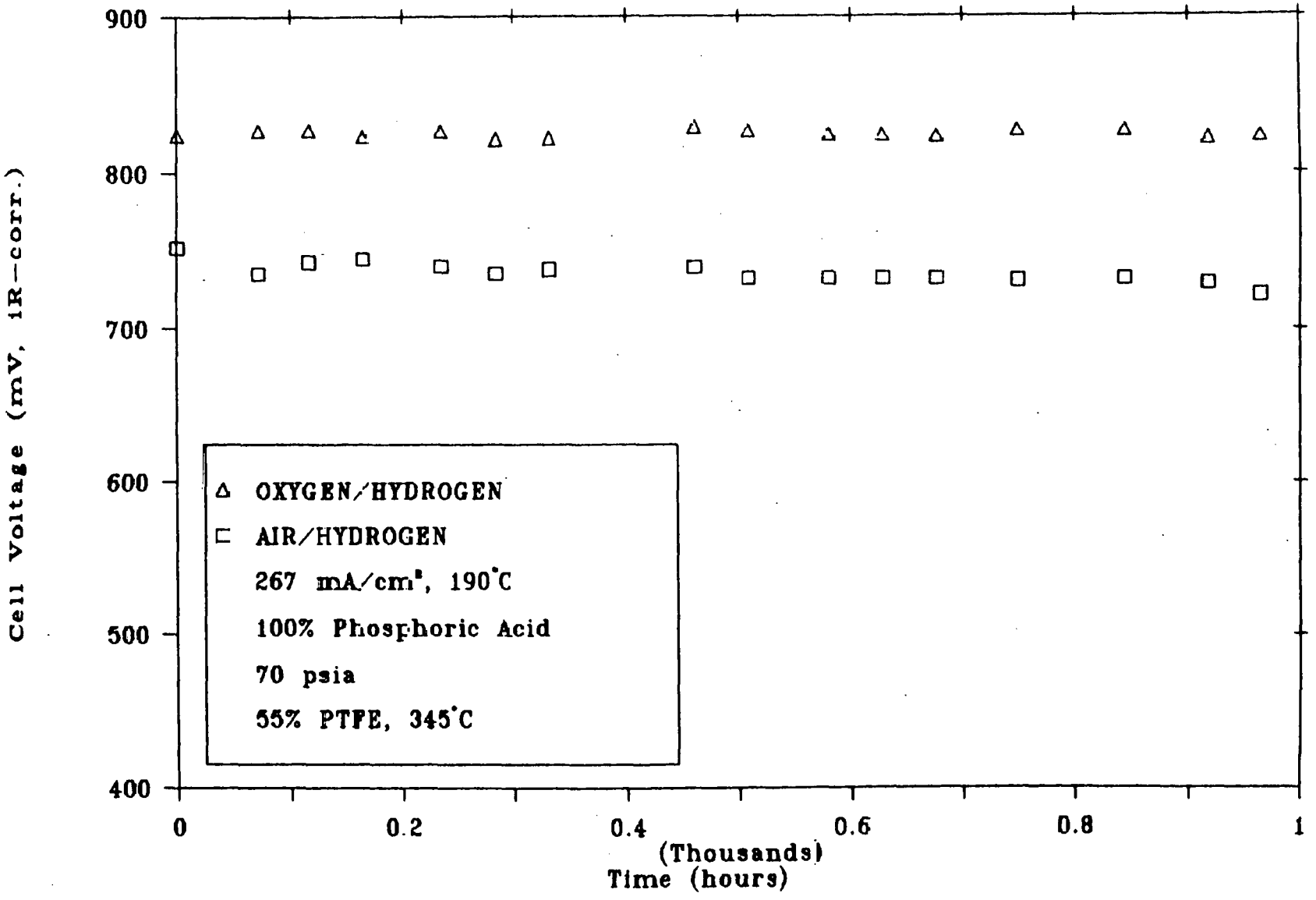

Figure 6-10. Life Performance of a Fuel Cell Containing the Pt-Ni-Co/HTBP Electrocatalyst During Pressurized Operation (Build 153)

6.4 OXIDE-FREE ELECTROCATALYSTS

6.4.1 Introduction

As described previously in Section 3, during the course of this program, evidence was obtained from Lawrence Berkeley Laboratory suggesting substantial amounts of base metal oxides were present in our platinum alloy electrocatalysts. The role of these metal oxides in the enhancement/degradation of alloy electrocatalyst activity, relative to that of unalloyed platinum, was unknown. Therefore, several approaches were evaluated to identify what role, if any, these oxides may play. The approaches included: (i) preparation of electrocatalysts containing substantial amounts of metal oxides, (ii) removal of metal oxides from standard electrocatalysts and (iii) preparation and evaluation of electrocatalysts by methods which avoid the formation of metal oxides.

6.4.2 Effect of Non-Heat-Treated Metal Oxides

Two variations of the Pt-Ni-Co electrocatalyst were prepared. The starting material in both cases was 900°C heat-treated platinized Vulcan XC-72, which was then impregnated with base metal oxides in the usual manner. The resulting material was filtered and dried. A small portion was subjected to a 900°C heat-treatment for one hour in an inert atmosphere, and designated G82-5-67. Gas diffusion electrodes were fabricated from both the non-heat-treated and the -67 electrocatalyst and evaluated for cathode performance and surface area; samples of the powders of these materials were submitted for XRD analyses. Results of this testing are summarized in **Table 6-VIII**. Included for reference are similar results for Pt/Vulcan, 900°C heat-treated Pt/Vulcan, Pt-Ni-Co/Vulcan and non-heat-treated Pt-Ni-Co/Vulcan.

The purpose of this study was to investigate the effect of non-heat-treated alloying components on cathode performance. It has been suggested that the presence of the non-heat-treated alloying components, which are presumed to be in the form of either a hydrated metal oxide, or a metal hydroxide adsorbed on the support surface, contributes to improved electrocatalyst performance by acting as a flux for the wetting of platinum crystallites. Examination of Table 6-VIII demonstrates that, when comparing a non-heat-treated versus a heat-treated electrocatalyst (e.g., Pt/Vulcan versus HT Pt/Vulcan, non-HT Pt-Ni-Co versus HT Pt-Ni-Co, etc.), a performance improvement is always observed with the heat-treated electrocatalyst.

Also, comparison of Pt/Vulcan and non-heat-treated Pt-Ni-Co/Vulcan shows very similar performance for both, even in the presence of hydrated metal oxides. Obviously, the data suggest that performance improvements are observed only after 900°C heat-treatment, and that the presence of non-heat-treated base metal oxides does not contribute to improved performance.

TABLE 6-VIII

EFFECT OF NON-HEAT-TREATED ALLOYING COMPONENTS ON Pt-Ni-Co ELECTROCATALYST

Electrocatalyst	iR-Free Performance* at 200 mA/cm² (mV)			Surface Area (m^2/g)	Lattice Parameter (Å)
	O_2	Air	Gain		
Pt/Vulcan	745	685	60	130	3.918
900°C HT Pt/Vulcan	768	696	72	61	3.909
Non-HT (Ni-Co) on 900°C HT Pt/Vulcan	757	691	66	--	-----
900°C HT (Ni-Co) on 900°C HT Pt/Vulcan	766 783	706 727	60 56	44	3.827
Non-Heat-Treated Pt-Ni-Co/Vulcan	742 744	678 677	64 67	95	3.918
Pt-Ni-Co/Vulcan	801	740	61	76	3.840

***Test Conditions**: Floating Electrode Half-Cell, 100% H_3PO_4 at 200°C

Samples of the non-heat-treated Pt-Ni-Co electrocatalyst were examined by means of TEM; two different batches were analyzed. The striking feature visible for each batch was the distribution of the electrocatalyst on the support particles; the smaller support particles appear to have a higher electrocatalyst loading than the larger support particles. Also, the electrocatalyst particles appear to congregate in crevices between the support particles.

Pre- and post-test half-cell electrodes fabricated from non-heat-treated Pt-Ni-Co electrocatalyst were also examined by use of TEM. The pre-test electrodes, except for the presence of added PTFE, were very similar to the non-heat-treated powders described above. Samples from the post-test electrodes, however, were significantly different.

The average pre-test particle size was on the order of 25 Angstroms with a non-uniform electrocatalyst spatial distribution influenced by the support particle size distribution. Average particle size of the post-test sample had increased to 50 Å. There was still a non-uniform electrocatalyst spatial distribution, but the loading was random and the influence of support size distribution was not present. Evidently, sintering of the electrocatalyst particles had occurred during the time frame of the half-cell testing.

6.4.3 Removal of Metal Oxides

An alternative method of preparing oxide-free electrocatalyst was to prepare electrocatalyst by the standard method, and then to remove any unalloyed (unreacted) excess metal oxides. Three methods were evaluated to remove excess metal oxides from the Pt-Ni-Co electrocatalyst; these tests are described below.

6.4.3.1 H_2SO_4 Reflux

The first method used for removal of excess metal oxides was an acid reflux. Several experiments using the Pt-Ni-Co/HTBP powder only (no PTFE present) were performed.

In the first experiment, boiling 18N H_2SO_4 was used to remove metal oxides from the electrocatalyst. Three separate acid leaches were performed, with each one lasting 6-7 hours; fresh acid was used for each run, while the electrocatalyst powder was not changed. Samples of both the powder and acid were analyzed for metal content after each leach. Results of this test are summarized in **Table 6-IX**.

TABLE 6-IX

RESULTS OF H_2SO_4 LEACH

Total Reflux Time (Hours)	Electrocatalyst Analysis (%) Pt	Ni	Co	Acid Analysis (ppm) Pt	Ni	Co
Initial	9.08	0.55	0.55	---	---	---
7	8.72	0.26	0.29	1.3	35.1	34.2
13.5	8.53	0.22	0.23	0.1	3.6	2.8
19.5	8.76	0.19	0.20	0.6	2.3	2.0

The major loss of Ni and Co occurred during the first leach with approximately 50% of the Ni and Co being removed. However, the ratio of Ni:Co in all leached powders was the same as the Ni:Co ratio of the starting material. The amounts of Ni and Co detected in the acid after the second leach were an order of magnitude lower than those detected after the first leach, while the amounts found after the third leach were almost identical to those found after the second leach.

A second, similar experiment was performed. This time, the Pt-Ni-Co/HTBP electrocatalyst was only refluxed for 7 hours, since most of the material was leached out during this time period. Three separate leaches were performed, using fresh acid and electrocatalyst for each; the first in air saturated 18N H_2SO_4 and the second while bubbling 5% H_2/N_2 through the boiling 18N H_2SO_4 (to protect the Pt from dissolution). The third was identical to the second, except non-heat-treated (unalloyed) electrocatalyst powder was used. This sample was run as a control to determine the extent of unalloyed metal dissolution.

Results of this test are summarized in **Table 6-X**, and are in agreement with those listed in Table 6-IX, in which an approximately 50% reduction in the percentage of Ni and Co was observed after the first 7-hour leach. The presence of H_2 appears to have protected the Pt somewhat; the H_2SO_4 Pt content of the acid leach conducted under a protective 5% H_2/N_2 atmosphere was 0.6 ppm while the acid leach conducted in ambient air resulted in 2.8 ppm Pt in the acid. Results obtained with the unalloyed electrocatalyst were significantly different. Now, more than 95% of the Ni and Co were found in the H_2SO_4, as opposed to the 50% seen for the alloyed electrocatalyst. However, very little platinum was found in solution. These data suggested that the Ni and Co oxides were extremely soluble in hot H_2SO_4 and that the solubility of the platinum alloy, at hydrogen potentials, was very limited. One can infer from these data that approximately 50% of the base metal oxides, originally precipitated onto the platinized support to form the platinum alloy, did not react.

The acid refluxed alloy electrocatalysts from above were fabricated into gas diffusion electrodes and evaluated for cathode activity in the floating electrode half-cell apparatus and for surface area. Samples of acid-refluxed powder were also sent out for XRD analyses. Results from these tests are summarized in **Table 6-XI**. Also included in this table are results obtained using a typical batch of Pt-Ni-Co/HTBP electrocatalyst.

TABLE 6-X

ANALYTICAL RESULTS

Sample	Electrocatalyst Analysis (%) Pt	Ni	Co	Acid Analysis (ppm) Pt	Ni	Co
I. H_2SO_4 Reflux						
Initial G82-5-75E	10.14	0.61	0.60	--	--	--
-75E Refluxed in H_2SO_4/Air	9.63	0.24	0.31	2.8	35	30
-75E Refluxed in H_2SO_4/H_2	9.45	0.29	0.25	0.6	32	26
II. H_2SO_4 Reflux Unalloyed Sample						
Initial G82-5-75F	10.81	0.50	0.51	--	--	--
-75E Refluxed in H_2SO_4/H_2	10.39	<0.007	<0.007	1.0	69	68

TABLE 6-XI

CHARACTERIZATION TESTING, ACID-LEACHED ELECTROCATALYST

Acid/Atmosphere	iR-Free Performance* at 200 mA/cm² (mV) O_2	Air	Surface Area (m^2/g)	Lattice Parameter (Å)
H_2SO_4/Air	772	700	63	3.853
H_2SO_4/5% H_2/N_2	780	712	52	3.859
NONE	772	696	76	3.864

***Test Conditions**: Floating Electrode Half-Cell, 100% H_3PO_4 at 200°C

Leaching the electrocatalyst powder and removal of excess metal oxides does not appear to have any effect on performance of the electrocatalyst. The only noticeable differences between the leached and the standard electrocatalyst are in the surface areas, where those of the acid-leached materials are slightly lower. This may be due to the dissolution of platinum, which was known to occur.

6.4.3.2 H_3PO_4 Dissolution

Testing similar to that described above was conducted using concentrated, 200°C H_3PO_4. Initially, Pt-Ni-Co/HTBP powder was allowed to soak in the hot acid for two, one-week periods using fresh acid for each one-week test; samples of acid were obtained and analyzed at the end of each week. Subsequent to the two, one-week tests, another test was run, but only for a 15-hour period, using a different batch of electrocatalyst.

Results of these tests are summarized in **Table 6-XII**. The solution platinum content from the 15 hour test appears high; it is suspected this was due to improper protection of the electrocatalyst by the 5% H_2/N_2 mixture. Acid leaches conducted with H_2SO_4, described above, using both air and 5% H_2/N_2 atmospheres demonstrated that the Ni and Co levels were only 9-13% higher in the air saturated solutions, while the Pt levels were 79% higher in the air saturated solutions. The Ni and Co levels observed in the 15-hour test suggest these components are initially removed very rapidly, with approximately 60% of the amount observed after a one-week leach seen after only 15 hours. The amount of Ni and Co observed in the solution after the second, one-week leach was very small. This demonstrated that any unalloyed metal oxides are removed from the electrocatalyst within the first week of contact with hot, concentrated phosphoric acid.

TABLE 6-XII

RESULTS OF H_3PO_4 LEACH*

Time	ppm Pt	ppm Ni	ppm Co
15 hours	27	61	62
First 1-week test	2	104	101
Second 1-week test	0.5	0.6	2

***Note:** Fresh acid used for each test

6.4.4. Electrocatalyst Characterization with ESCA

The standard Giner, Inc. alloy electrocatalyst preparation technique involves deposition of base metal oxides onto a platinized support, followed by heat-treatment to effect alloy formation. Electron spectroscopy for chemical analysis (ESCA) was used to determine the chemical state of the metal components of the electrocatalysts. The materials examined were 900°C HT Pt/Vulcan, 900°C HT Pt-Ni-Co/Vulcan and non-HT Pt-Ni-Co/Vulcan.

Due to the very low Ni and Co content in the electrocatalyst, it was extremely difficult to differentiate between metallic Ni and Ni-oxide and between metallic Co and Co-oxide in the 900°C HT Pt-Ni-Co/Vulcan sample. Therefore, a definite statement concerning the chemical state of Ni and Co cannot be made. However, the presence of each was observed in the sample of 900°C HT Pt-Ni-Co/Vulcan. The small quantities of Ni and Co approached the detection limits of the instrument.

Therefore, because only strong Pt signals were obtained, we decided to concentrate on analyzing the Pt and Pt oxide peaks of the three samples. These results were extremely subjective and showed a strong dependence on the instrumental conditions used in obtaining the ESCA spectra. Both low and high resolution scans were recorded for the Pt peaks of all three samples; the magnitude and spacing of the Pt peaks shifted, going from low to high resolution. Standard curve fitting was performed on the high resolution peaks to separate out the contributions due to Pt and Pt oxide. The results, summarized in **Table 6-XIII**, were dependent upon parameters introduced into the curve fitting algorithms. For example, forcing the width of the peaks, at half the maximum height, to remain at 2 eV resulted in Pt to $Pt(OH)_2$ ratios which suggested the non-HT Pt-Ni-Co/Vulcan sample contained the most $Pt(OH)_2$, while the 900°C HT Pt-Ni-Co/Vulcan had the least oxide. Allowing the full widths at half-height to vary resulted in the exact opposite order.

TABLE 6-XIII

ESCA CURVE FITTING RESULTS

Sample	$Pt/Pt(OH)_2$* Ratio	$Pt/Pt(OH)_2$** Ratio
900°C Pt	2.09	2.42
Pt-Ni-Co/Vulcan	3.88	1.97
Non-HT Pt-Ni-Co/Vulcan	1.99	2.7

* Forcing full width half max = 2 ev
** Allowing full width half max to vary

The results of this work were extremely dependent upon the experimental conditions employed while obtaining the data, and also extremely dependent on the algorithms utilized for data reduction. Therefore, no definite conclusions could be made.

6.4.5 Base Metal Sulfide Preparation

The standard Giner, Inc. electrocatalyst preparation method was modified to precipitate both nickel and cobalt as sulfides instead of hydrated oxides. Initial testing was performed using Vulcan as a support; subsequent and more extensive preparations were conducted using the HTBP support. **Table 6-XIV** compares characterization data for Pt-Ni-Co electrocatalysts prepared by both the oxide and sulfide methods.

TABLE 6-XIV

COMPARISON OF Pt-Ni-Co ELECTROCATALYSTS PREPARED BY BOTH SULFIDE AND OXIDE METHODS

Method	iR-Free Performance* at 200 mA/cm² (mV)		Surface Area (m²/g)
	O_2	Air	
Sulfide	773	703	66
Oxide	801	740	60-70

***Test Conditions:** Floating Electrode Half-Cell, 100% H_3PO_4 at 200°C

Although performance of the electrocatalyst prepared by the sulfide method was lower than that of electrocatalyst prepared by our standard method, the results were extremely encouraging. In our initial attempt at sulfide method electrocatalyst preparation, we were able to obtain performance reasonably close to that observed for electrocatalyst prepared using our optimized standard procedure. The surface area of the sulfide electrocatalyst was 66 m²/g, which fell into the same range (60-70 m²/g) observed for electrocatalyst prepared by the standard method.

A large batch of Pt-Ni-Co/HTBP electrocatalyst was prepared by the sulfide method, separated into 8 smaller batches, and heat-treated at 500, 700, 900 and 1100°C in hydrogen for either 1 or 2.5 hours (with the exception of the material heat-treated at 500°C for 2.8 hours). Weight losses during heat-treatment were measured and summarized in **Table 6-XV**.

The weight change during the heat-treatment showed little variation with the time or temperature for 500 and 700°C. The materials heat-treated at 900 and 1100°C each showed an increase in the magnitude of the weight change with time. The comparable weight

changes from heat-treatment at 900 and 1100°C for 2.5 hours may indicate that any impurities introduced during preparation have been removed. To verify the effect of heat-treatment time and temperature on electrocatalyst composition, selected samples were sent for elemental analysis. No differences in composition were observed.

TABLE 6-XV

WEIGHT CHANGE DURING HEAT-TREATMENT

Temperature (°C)	Weight Change After 1 Hour	Weight Change After 2.5 Hours
500	-8.4%	-8.2%*
700	-8.6%	-8.9%
900	-11.4%	-14.6%
1100	-12.3%	-14.3%

* After 2.8 hours

Electrodes were fabricated from each of the electrocatalyst batches and tested using the floating electrode half-cell apparatus. The results are given in **Table 6-XVI**. Results for the Pt-Ni-Co/HTBP electrocatalyst prepared by the standard method are included for comparison.

TABLE 6-XVI

HALF-CELL PERFORMANCE OF ELECTROCATALYST PREPARED BY THE SULFIDE METHOD

Heat-Treatment Temperature (°C)	Time (Hours)	iR-Free Performance* at 200 mA/cm² (mV)		Surface Area (m²/g)		Average Diameter (Å)
		O_2	Air	TEM	EC	
500	1	742	662	74	76	38
700	1	757	677	67	60	42
900	1	767	690	56	51	50
1100	1	763	683	39	43	72
500	2.8	737	657	64	78	44
700	2.5	753	676	53	69	53
900	2.5	772	692	45	62	62
1100	2.5	770	683	37	56	76
900 Standard Pt-Ni-Co/HTBP	1	771	693	--	76	--

***Test Conditions**: Floating Electrode Half-Cell, 100% H_3PO_4 at 200°C

Data presented in Table 6-XVI shows that half-cell performance increased with increasing heat-treatment temperature, and peaked at 900°C; this effect has previously been seen with the Pt-Ni-Co/Vulcan electrocatalyst prepared by the standard method. Longer heat-treatment time did not have any significant effect on performance. However, as also shown in Table 6-XVI, longer heat-treatment led to an increase in surface area.

All electrocatalysts prepared by the sulfide method were examined using TEM. The average particle size and the surface area, assuming spherical catalyst particles, are also in Table 6-XVII. Surface area data in this table demonstrate the effect of heat-treatment time. For the 1-hour heat-treated electrocatalyst, TEM surface areas were larger than the electrochemical surface areas, while the opposite effect was observed for the 2.5-hour heat-treatment time. The longer heat-treatment time at a given temperature led to an increase in the electrochemically active surface area due to the removal of hydrogen-adsorption-blocking impurities such as sulfur.

6.5 *CONCLUSIONS*

The following conclusions can be drawn from the work presented in this chapter:

1. A high activity platinum ternary alloy electrocatalyst having an optimum starting Pt-Ni-Co atomic ratio of 70:15:15 was developed and patented.

2. The optimum heat-treatment temperature for electrocatalyst preparation was 900°C; use of an ultra-pure inert atmosphere for heat-treatment was not required.

3. Removal of excess metal oxides does not degrade electrocatalyst performance.

4. Using Pt-Ni-Co/HTV, 10,000 hours of stable fuel cell performance at atmospheric conditions can be obtained.

5. Demonstrated 1,000 hours of stable fuel cell performance at pressurized conditions using both Pt-Ni-Co/HTV and Pt-Ni-Co/HTBP.

6. New preparation methods for high activity electocatalysts were identified.

7.0 DISCUSSION

7.1 ACTIVITY ENHANCEMENT

7.1.1 Introduction

A number of theories have been proposed to explain the enhancement in electrocatalytic activity, with respect to platinum, due to alloying. Among these are (i) "Raney" platinum precursor, (ii) Metal oxide flux, (iii) Heat-treatment and the resulting change in crystallinity and (iv) Nearest-neighbor distance. These will be discussed below, with reference to data presented in Sections 5.0 and 6.0 of this report.

7.1.2 "Raney" Platinum Precursors

The preparation of high surface area metals by the Raney method is well known. An easily removable material such as aluminum is alloyed with another metal. The aluminum is subsequently dissolved in a solvent such as KOH leaving a high surface area form of the starting material. The removal of Cr from bulk Pt-Cr alloys, resulting in increased Pt surface area, has been proposed as an explanation for enhanced electrocatalytic activity (1).

A similar procedure could be happening to our Pt-Ni-Co electrocatalysts, whereby the Ni and Co both dissolve in hot, concentrated phosphoric acid, leaving a platinum crystallite whose surface area is increased due to the presence of minute "craters", left from the dissolution of nickel and cobalt. However, based on our acid dissolution results, this theory does not seem plausible. We found that approximately 50% of the nickel and cobalt initially deposited on the electrocatalyst surface could be removed through acid dissolution with no effect on half-cell performance. In addition, no change in electrochemically active surface area, measured by hydrogen adsorption, was observed for the electrocatalyst refluxed in acid.

Therefore, we can conclude that activity enhancement is not due to the presence of a Raney platinum precursor.

7.1.3 Metal Oxide Flux

Another theory proposed for activity enhancement in alloy electrocatalysts is the metal oxide flux theory. Substantial amounts of base metal oxides are supposedly present in our alloy

electrocatalysts. These metal oxides, when in contact with a platinum crystallite, can act as a flux and allow for easier wetting of the surface of the platinum crystallite, with a resulting increase in electrocatalytic activity (2).

Data obtained during the course of this program suggest that this theory does not adequately explain activity enhancement. Specifically, data on Pt-Ni-Co presented in Section 6.4.2 demonstrated that a performance improvement was obtained if, and only if, the electrocatalyst was subjected to a 900°C heat-treatment step. The presence of non-heat-treated nickel oxide and cobalt oxide did not have any effect on half-cell performance.

7.1.4 Heat-Treatment and Change in Crystallinity

Another explanation for the increase in performance with alloy formation is that the heat-treatment of platinum microparticles in the presence of metal oxides not only produces platinum alloys, but also causes a significant change in the crystallinity of the electrocatalyst.

It has been shown that platinum particle size increase by electrochemical sintering gave higher activity and higher Tafel slope (3) with a resulting net loss in the performance. However, particle size increase by a 900°C heat-treatment of the Pt/Vulcan electrocatalyst resulted in improved oxygen reduction performance, presumably due to more favorable crystallinity (4). Transmission electron micrographs were obtained for four different materials: as-prepared Pt/Vulcan, electrochemically aged Pt/Vulcan, 900°C heat-treated Pt/Vulcan and 1050°C heat-treated Pt/Vulcan. While the particle sizes of the electrochemically sintered (1200 hours at 700 mV in 100% H_3PO_4 at 200°C) and thermally sintered (at 1050°C) platinum were approximately the same, clustering of the platinum in a chain-like form was observed in the case of the former. This was also observed in studies of an electrochemically sintered model catalyst (5). In contrast, the thermally sintered platinum was rather uniformly dispersed. At higher sintering temperatures, although the platinum crystallites were still discrete, the appearance of the hexagonally-shaped particles suggested a change in crystallinity.

Fuel cell testing has shown that this performance improvement of the 900°C heat-treated platinum versus the non-heat-treated platinum persisted over a 10,000-hour test. Comparison of the surface areas of platinum and heat-treated platinum during this life test showed that,

although the initial surface area of the non-heat-treated platinum was much higher, the rate of decrease in surface area was also higher than that of the heat-treated material.

Heat-treatment of the platinum/Vulcan electrocatalyst at temperatures higher than 900°C resulted in an even larger platinum particle size, which the net result being a decrease in performance. This performance loss appeared to be due to excessive surface area loss. It may be postulated that the heat-treatment of platinum in the presence of metal oxide produced a crystalline electrocatalyst which was more active for oxygen reduction than its precursor amorphous, microparticles of platinum (6, 7).

7.1.5 Nearest-Neighbor Theory

The nearest-neighbor theory (8) states there is an optimum interatomic spacing between sites at which an oxygen molecule is adsorbed prior to bond rupture. At larger than optimum spacing, dissociation would have to occur prior to adsorption and at a smaller than optimum spacing, repulsive forces would retard the dual site oxygen-oxygen bond breaking. A plot of electrocatalyst activity versus nearest-neighbor distance, presented as Figure 5-3, resulted in a linear relationship, with the highest specific activity resulting from the electrocatalyst with the smallest nearest-neighbor distance.

The nearest-neighbor distance theory predicted that an electrocatalyst having a nearest-neighbor distance less than that observed for Pt-Cr should result in increased oxygen reduction activity. The Pt-Ni-Co ternary platinum alloy, with a nearest-neighbor distance less than that of Pt-Cr, had an activity increase of 20 mV (at 200 mA/cm^2) relative to that of Pt-Cr.

7.2 STABILITY CONSIDERATIONS

The design goal for PAFC power plants currently under development by Westinghouse and others is an overall voltage decay rate of -2 mV/1000 hours of operation, over a projected 40,000-hour fuel cell lifetime. Fuel cell life plots, presented in Section 6.0, demonstrated that, over periods from 1,000 to 10,000 hours, the Pt-Ni-Co electrocatalyst is capable of stable performance under both atmospheric and pressurized operating conditions. An overall decay rate, from peak performance, of -4 mV/1000 hours was observed during a 10,000-hour life test of the Pt-Ni-Co/HTV electrocatalyst.

The stability of the cathode electrocatalyst will be determined by the stability of both the electrocatalytic crystallites and also the stability of the electrocatalyst support itself. **Figure 7-1** shows corrosion currents of three different electrocatalyst supports, two graphitic and one non-graphitic, measured over a 1,000-minute period under simulated pressurized fuel cell operating conditions. The measured corrosion currents of HTV and HTBP were both at least a factor of 2 lower than that of Vulcan. Therefore, both HTV and HTBP would be viable electrocatalyst supports to be used in pressurized fuel cell operation.

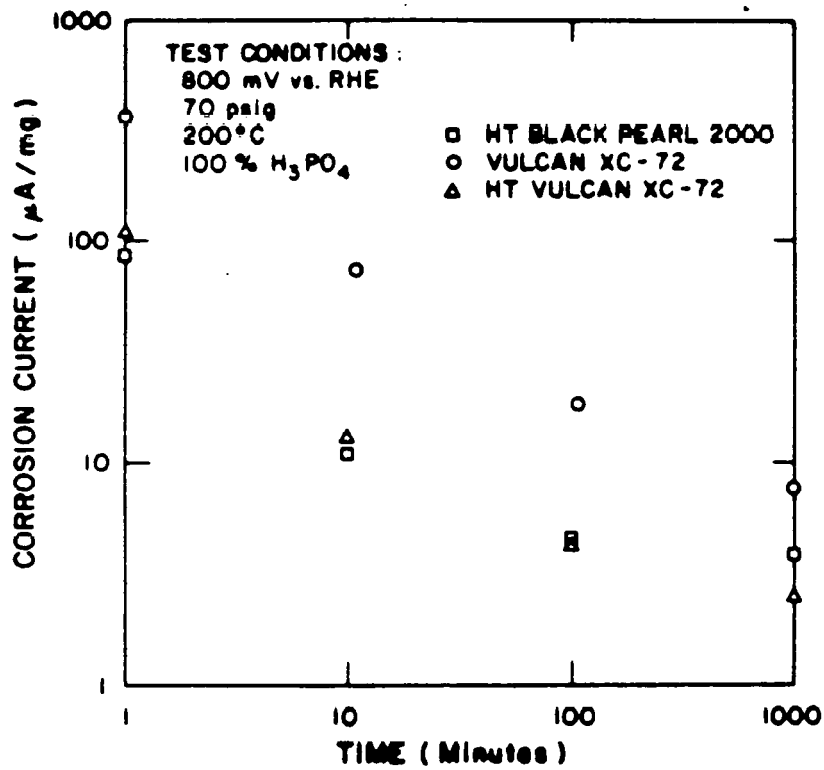

Figure 7-1. Corrosion Currents of Various Electrocatalyst Supports

The stability of the electrocatalytic particles dispersed on the support is dependent, to some extent, on the structure and composition of the electrocatalyst. Despite extensive study of the effects of several preparation parameters, the precise composition and structure of the electrocatalyst, as prepared on a carbon support, are not yet known. The electrocatalyst is prepared by precipitating the hydroxides of nickel and cobalt onto carbon powder which already supports a high surface area platinum catalyst. This mixture of hydroxides, platinum and carbon is subjected to a heat-treatment which decomposes

the hydroxides and promotes alloying of the metal components: platinum, nickel, and cobalt. After heat-treatment, the electrocatalyst may consist of any or all of the following:

- Metallic alloys of Pt particles as Pt-Co, Pt-Ni, Pt-Ni-Co of various compositions and structures (intermetallic or solid solution).
- Unalloyed Pt particles
- Unreacted metal oxides, CoO_x, NiO_x
- Reduced metallic components Co, Ni
- Mixed oxides of Pt such as $PtCoO_x$, $PtNiO_x$, $PtNi_xCo_yO_z$ in spinel, bronze, perovskite, pyrochlore, or other structures.

Analysis of the catalyst by EXAFS and XPS techniques has shown the presence of nickel oxide (9). It is not known whether this oxide was isolated from any platinum-containing catalyst particles, whether it was intimately associated with them or whether it was part of a platinum-based mixed oxide compound. Neither is it known to what extent the catalyst particles are alloyed or whether the alloy formed is disordered or crystalline.

Microanalysis of electrocatalyst particles using scanning transmission electron microscopy/energy dispersive X-ray analysis (STEM/EDX) has shown the presence of nickel oxides, cobalt oxides and platinum oxide in individual electrocatalyst particles (10). Nickel and cobalt were not detected on the carbon support in between electrocatalyst crystallites. This suggested that any cobalt or nickel on the carbon support itself was present at a level much below that on, or in, the platinum crystallites. The nickel or cobalt content on the carbon support must be ≤ 0.33 that on platinum, otherwise a signal would have been detected. However, the extent to which the electrocatalyst particles were alloyed or whether the alloy formed was disordered or crystalline was again not known. Evidence presented in Section 6 of this report also confirmed the existence of platinum oxide from ESCA analysis.

Acid dissolution experiments, described in Section 6, removed approximately 50% of the nickel and cobalt originally present in the electrocatalyst. Floating electrode half-cell testing of the acid-washed electrocatalyst showed no loss in performance, compared to unwashed electrocatalyst. These results suggested we had removed either unreacted metal oxides (NiO_x and CoO_x) or reduced metallic components (Ni, Co).

XRD data obtained on the Pt-Ni-Co electrocatalyst, along with our one-hour, 900°C heat-treatment, suggest the formation of solid solutions, rather than intermetallic compounds. The absence of superlattice lines in the XRD patterns is also evidence for solid solutions, rather than intermetallic formation. However, the diffuse patterns obtained due to the low metal loadings (10 wt% metal, 90 wt% carbon) and small particle size (40-60 Å), may make superlattice lines difficult to detect. Phase diagrams for Pt-Ni and Pt-Co show complete solid solubility over the temperature and composition ranges which we are using for alloy formation (10).

7.3 CONCLUSIONS

The following conclusions can be made based on the above work:

1. The enhancement in electrocatalytic activity due to alloy formation appears to be related to both a change in crystallinity due to heat-treatment, and activity enhancement predicted by the nearest-neighbor distance theory.

2. Characterization evidence suggests our alloys are solid solutions, and not intermetallics, with base metal oxides present.

3. Corrosion currents of graphitized electrocatalyst supports are lower than those of non-graphitized supports.

7.4 REFERENCES FOR SECTION 7.0

1. Daube, K.A., M.T. Paffett, S. Gottesfeld and C.T. Campbell, *J. Vac. Sci. Technol. A*, **4**, 1617 (1986).

2. Ross, P.N. and A.J. Appleby, paper presented at 188th ACS Meeting, Philadelphia, PA (August, 1984).

3. Bregoli, L.J., *Electrochim. Acta*, **23**, 489 (1978).

4. Jalan, V., E.J. Taylor, M. Desai and B. Morriseau, Extended Abstracts, Vol. 84-2, The Electrochemical Society, Pennington, N.J. (1984).

5. Jalan, V., "Substitutes for Carbon in Fuel Cell Applications," in Proceedings of the Workshop on the Electrochemistry of Carbon, S. Sarangapani, J.R. Akridge, B Schuman (Eds.), The Electrochemical Society (1983).

6. Jalan, V. and P. Stonehart, Extended Abstracts, Vol. 79-2, The Electrochemical Society, Pennington, N.J. (1979).

7. Jalan, V., Extended Abstracts, Vol. 82-1, The Electrochemical Society, Pennington, N.J. (1982).

8. Jalan, V. and E.J. Taylor, *J. Electrochem. Soc.*, **130**, 2299 (1983).

9. Ross, P.N., Lawrence Berkley Laboratory, private communication.

10. Vander Sande, J., MIT, private communication.

8.0 RECOMMENDATIONS FOR FUTURE RESEARCH

1. The platinum ternary alloy electrocatalyst, Pt-Ni-Co, supported on corrosion resistant supports such as HTV and HTBP, has shown considerable promise for use as a cathode catalyst in a PAFC. It is recommended that long-term stability tests be conducted to verify the stability of the materials over extended (>10,000 hours) periods of time.

2. Despite extensive research, the precise composition and structure of the Pt-Ni-Co alloy is unknown. It is recommended that use be made of the sophisticated analytical tools at the National Laboratories, such as EXAFS, to further characterize this material.

3. Analyses of electrodes and electrode packages by techniques such as X-ray Photoelectron Spectroscopy (XPS) and Rutherford Backscattering Spectroscopy (RBS) at Los Alamos National Laboratory could provide characterization and stability information on the Pt-Ni-Co system; it is recommended such analyses be conducted.

4. The use of alternative electrocatalyst preparation procedures has resulted in material supported on corrosion-resistant supports having performance approaching that of Pt-Ni-Co/Vulcan. Therefore, further research into alternative preparation procedures is recommended.

5. Microanalysis of individual electrocatalyst particles has yielded preliminary information concerning the chemical composition of Pt-Ni-Co crystallites. Further research is required to identify the various metal and metal oxide phases which may be present.

6. Variations in electrocatalyst performance have been observed depending on the electrocatalyst support used. Typically, the highest performance has been observed for electrocatalyst systems supported on Vulcan XC-72, and lower performance on graphitized supports. Therefore, further research is recommended in the areas of electrocatalyst/support interaction and support stability.